White Rose Research Online

eprints@whiterose.ac.uk
https://eprints.whiterose.ac.uk
Universities of Leeds, Sheffield and York

Deposited via The University of Leeds.

White Rose Research Online URL for this paper:
https://eprints.whiterose.ac.uk/id/eprint/142229/

Version: Accepted Version

**Article:**
Förster, S, Schmidt, LK, Kopic, E et al. (2019) Wounding-Induced Stomatal Closure Requires Jasmonate-Mediated Activation of GORK K+ Channels by a Ca2+ Sensor-Kinase CBL1-CIPK5 Complex. Developmental Cell, 48 (1). 87-99.e6. ISSN: 1534-5807

https://doi.org/10.1016/j.devcel.2018.11.014

© 2018 Elsevier Inc. This manuscript version is made available under the CC-BY-NC-ND 4.0 license http://creativecommons.org/licenses/by-nc-nd/4.0/.

**Reuse**
This article is distributed under the terms of the Creative Commons Attribution-NonCommercial-NoDerivs (CC BY-NC-ND) licence. This licence only allows you to download this work and share it with others as long as you credit the authors, but you can't change the article in any way or use it commercially. More information and the full terms of the licence here: https://creativecommons.org/licenses/

**Takedown**
If you consider content in White Rose Research Online to be in breach of UK law, please notify us by emailing eprints@whiterose.ac.uk including the URL of the record and the reason for the withdrawal request.

UNIVERSITY OF LEEDS
University of Sheffield
UNIVERSITY of York

# Wounding induced stomatal closure requires Jasmonate dependent activation of the GORK $K^+$ efflux channel via $Ca^{2+}$ sensor-kinase CBL1-CIPK5 complexes

Sabrina Förster[1,8,@], Lena K. Schmidt[2,@], Eva Kopic[1,@], Uta Anschütz[1], Shouguang Huang[1], Kathrin Schlücking[2,3], Philipp Köster[2], Rainer Waadt[4], Antoine Larrieu[5,9], Oliver Batistič[2], Pedro L. Rodriguez[6], Erwin Grill[7], Jörg Kudla[2], and Dirk Becker[1,10,*]

[1] Molekulare Pflanzenphysiologie & Biophysik, Julius-Maximilians-Universität Würzburg, Julius-von-Sachs-Platz 2, 97082 Würzburg, Germany
[2] Institut für Biologie und Biotechnologie der Pflanzen, Westfälische Wilhelms-Universität Münster, Schlossplatz 7, 48149 Münster, Germany
[3] Present address: Botanisches Institut, Universität zu Köln, Zülpicher Str. 47b, 50674 Köln, Germany
[4] Centre for Organismal Studies, Ruprecht-Karls-Universität Heidelberg, Im Neuenheimer Feld 230, 69120 Heidelberg, Germany
[5] Laboratoire Reproduction et Développement des Plantes, Univ Lyon, ENS de Lyon, UCB Lyon 1, CNRS, INRA, 69342, Lyon, France
[6] Instituto de Biologia Molecular y Celular de Plantas, Consejo Superior de Investigaciones Cientificas-Universidad Politecnica de Valencia, 46022 Valencia, Spain
[7] Lehrstuhl für Botanik, Technische Universität München, Emil-Ramann Straße 4, 85354 Freising, Germany
[8]present address: Department of Plant Molecular Biology, University of Lausanne, 1015 Lausanne, Switzerland
[9]present address: Centre for Plant Sciences, University of Leeds, Leeds LS2 9JT, UK
[10]Lead Contact

[@] contributed equally to this work
[*] Correspondence
dirk.becker@uni-wuerzburg.de

**Summary**

Guard cells integrate various hormone signals and environmental cues to balance plant gas exchange and transpiration. The wounding-associated hormone jasmonic acid (JA) and the drought hormone abscisic acid (ABA) both trigger stomatal closure. In contrast to ABA however, the molecular mechanisms of JA-induced stomatal closure have remained largely elusive. Here, we identify a fast signaling pathway for JA targeting the $K^+$ efflux channel GORK. Wounding triggers both local and systemic stomatal closure by activation of the JA signaling cascade followed by GORK phosphorylation and activation through CBL1-CIPK5 $Ca^{2+}$ sensor-kinase complexes. GORK activation strictly depends on plasma membrane targeting and $Ca^{2+}$ binding of CBL1-CIPK5 complexes. Accordingly, in *gork*, *cbl1* and *cipk5* mutants, JA-induced stomatal closure is specifically abolished. The ABA-coreceptor ABI2 counteracts CBL1-CIPK5 dependent GORK activation. Hence, JA-induced $Ca^{2+}$ signaling in response to biotic stress converges with the ABA mediated drought stress pathway to facilitate GORK-mediated stomatal closure upon wounding.

**Keywords**: Guard Cell, Jasmonic Acid, Abscisic Acid, Wounding, Calcium, Potassium Channel

**Introduction**

Balancing $CO_2$ uptake with transpiration (i.e. water use efficiency) relies on tightly controlled turgor changes in the two guard cells, which form the stomatal pores in the leaf epidermis (Roelfsema and Hedrich, 2005; Schroeder et al., 2001). Guard cells respond to numerous exogenous and endogenous cues such as $pCO_2$, humidity, light and microbial elicitors, as well as signaling hormones including abscisic acid (ABA) and jasmonate (JA) (Murata et al., 2015; Bauer et al., 2013; Melotto et al., 2008; Hetherington, 2001). While drought stress triggers ABA biosynthesis and signaling, pathogen attack or herbivore mediated wounding result in increased JA levels and activation of JA signaling (Mousavi et al., 2013; Gfeller et al., 2010; Glazebrook, 2005). Both hormones trigger specific downstream responses upon interaction with their specific receptors, represented by the PYR/PYL/RCAR (PYRABACTIN RESISTANCE LIKE, REGULATORY COMPONENT OF ABA RECEPTOR) family for ABA and COI1 (CORONATINE INSENSITIVE 1) for JA (Raghavendra et al., 2010; Yin, et al., 2009). During drought stress-induced stomatal closure, ABA binding stabilizes protein complexes consisting of PYR/PYL/RCAR proteins and its PP2C (PROTEIN PHOSPHATASE 2) co-receptor. This leads to inhibition of PP2C activity of the prominent guard cell phosphatases ABA-INSENSITIVE 1 and 2 (ABI1 and 2). Consequently, ABA-mediated inhibition of PP2C activity releases inhibition of the protein kinase OST1 (OPEN STOMATA 1). As a positive regulator in guard cell ABA signaling, OST1 phosphorylates target proteins including guard cell anion efflux channels of the SLAC1/SLAH family (SLOW ANION CHANNEL-ASSOCIATED 1/HOMOLOGOUS; Hedrich and Geiger, 2017; Geiger et al., 2009). OST1 triggered activation of SLAC1 leads to guard cell membrane potential depolarization (Maierhofer et al., 2014; Imes et al., 2013; Vahisalu et al.,

2008). Both OST1-dependent inhibition of the guard cell $K^+$ uptake channel KAT1 (Yin et al., 2016) and membrane potential depolarization appear to be crucial for enhancing $K^+$ efflux from guard cells, mediated by the GUARD CELL OUTWARD-RECTIFYING $K^+$ channel (GORK) (Hedrich and Geiger, 2017; Hosy et al., 2003; Ache et al., 2000). The concomitant efflux of anions and potassium reduces guard cell turgor, resulting in stomatal closure (Hedrich, 2012). Like ABA, the wounding hormone JA represents a well-known trigger of stomatal closure (Murata et al., 2015) and a role for JA has recently been discussed in the light of stomatal contribution to plant innate immunity and elevated $CO_2$ (Geng et al., 2016; McLachlan et al., 2014; Montillet and Hirt, 2013; Sawinski et al., 2013; Melotto et al., 2008). In addition, oxylipin and JA biosynthesis and signaling seem to control herbivore induced reduction in photosynthesis (Meza-Canales et al., 2017; Nabity et al., 2013). The molecular players involved in this process, shifting plant metabolism from growth to defense, are largely unknown. Both ABA and JA induce specific $Ca^{2+}$ signatures in guard cells (Islam et al., 2010; Allen et al., 2001). $Ca^{2+}$ signals are decoded by an elaborate toolkit of $Ca^{2+}$ sensor proteins involving (among others) families of $Ca^{2+}$-dependent protein kinases (CDPKs, in Arabidopsis designated as CPKs) and CALCINEURIN B-LIKE PROTEINS (CBLs), which interact with CBL-INTERACTING PROTEIN KINASES (CIPKs; Hashimoto and Kudla, 2011). In a Xenopus oocyte-based functional screen the vascular expressed CPK33 was recently identified as a positive regulator of GORK (Corratge-Faillie et al., 2017). During ABA signaling CDPKs as well as CBL1/9-CIPK23 complexes phosphorylate and activate the guard cell anion channel SLAC1 (Maierhofer et al., 2014; Brandt et al., 2012; Scherzer et al., 2012). However, the mechanisms that bring about JA-induced stomatal closure remain largely elusive. In this study, we identify the guard cell $K^+$

efflux channel GORK as an integrative component of JA and ABA pathways, triggering stomatal closure and linking the carefully balanced activity of $Ca^{2+}$-activated $Ca^{2+}$-sensor-kinase complexes and an ABA-inactivated PP2C-type phosphatase to the convergence of JA and ABA signals at the channel protein.

## Results

### Wounding triggers JA signaling in stomatal guard cells

Playing an essential role in plant growth and development as well as defense responses JA biosynthesis and signaling is rapidly induced in response to wounding. JA has been implicated in promoting stomatal closure (Savchenko et al., 2014) but it is currently not known whether a wounding signal affects stomatal aperture. We therefore mechanically wounded leaves of Arabidopsis. Subsequent stomatal aperture assays revealed that stomata closed within 1.5h and were fully closed 2h after stimulus onset (Fig. 1A and VideoS1). Remarkably, stomatal closure did not only occur in wounded leaves (locally) but also in unwounded distal leaves (Fig. S1A). Reminiscent to wound induced electrical signaling triggering JA biosynthesis (Mousavi et al., 2013) this behavior suggests that wounding elicits JA signaling in guard cells. In order to follow JA signaling in guard cells we took advantage of the recently developed genetically encoded JA-biosensor Jas9-VENUS (Larrieu et al., 2015). In non-wounded leaves, no correlation was observed between Jas9-VENUS/H2B-RFP fluorescence ratios in guard cells and stomatal aperture (Fig. S2). This suggests that stomatal aperture in healthy leaves is most likely JA independent. Upon wounding induced closure however, guard cell Jas9-VENUS/H2B-

RFP fluorescence ratios declined rapidly (Fig. 1B and C), suggesting that activation of the guard cell JA signaling cascade precedes stomatal closure. The observation that wound induced stomatal closure as well as guard cell JA signaling was significantly impaired in the *coi1* mutant (Fig. S1B and C) further supports the idea that wounding addresses the canonical jasmonate pathway in guard cells.

**The guard cell $K^+$ efflux channel GORK operates specifically in JA-induced stomatal closure**

Patch clamp studies on *Vicia faba* guard cell protoplasts by Evans (2003) indicated that methyl jasmonate (MeJA) promotes potassium efflux. Two voltage dependent $K^+$ efflux channels are encoded in the Arabidopsis genome: the stelar expressed SKOR (STELAR K OUTWARD RECTIFIER) channel mediating $K^+$ release into the xylem sap and the guard cell expressed GORK (GUARD CELL OUTWARD RECTIFYING K CHANNEL; Anschütz et al., 2014; Ache et al., 2000). To investigate a possible role of GORK in JA-mediated fast stomatal closure we performed whole-cell patch-clamp recordings on guard cell protoplasts of Col-0 wild-type (wt) and *gork1-2* (GABI_865F05) mutants under asymmetric potassium conditions, with 100 mM and 10 mM $K^+$ in pipette and bath solutions. Starting from a holding potential of -60 mV voltage pulses in the range from -180 to 100 mV elicited large inward (-90±9 pA/pF at -160 mV) and small outward $K^+$ currents (13±1.7 pA/pF at 100 mV) under control conditions (Fig. 2A, left traces). While $K_{in}$ current density appeared high in the *gork1-2* mutant (-162±23 pA/pF at -160 mV), depolarization activated, $K_{out}$ currents were absent in the knockout (Fig. 2A, right traces, 1.7±0.6 pA/pF at 100 mV). To study the effect of JA on GORK regulation we treated guard cell protoplast with the JA-Ile mimic coronatine (COR; Sheard et al., 2010; Xie et al., 1998) rather

than volatile MeJA (see methods). Following a 15 min preincubation of guard cell protoplasts with COR we observed a significant increase (3.62±0.85x; $p<0.005$) in outward $K^+$ current density (Fig. 2B and C, left). This COR triggered $K_{out}$ channel activity was absent in the *gork1-2* mutant (Fig. 2B and C, right). In both wt and the *gork1-2* mutant the activity of inward rectifying $K^+$ channels was significantly reduced upon COR treatment (Yin et al., 2016). Together these results demonstrate that besides $K^+$ uptake channels, the GORK $K^+$ efflux channel represents a target of JA-signaling in guard cells. Investigating guard cell responses to exogenously applied MeJA or ABA in stomatal aperture assays corroborated this finding. This approach identified the *GORK* loss-of-function allele *gork1-2* as being specifically impaired in the JA response (Fig. 2D and E). In contrast, the mutant exhibited an almost wild type-like response to the *Pseudomonas* elicitor peptide flg22 and a partially impaired response to ABA (Fig. 2D and E; Fig. S3). The JA stoma phenotype appeared to occur independently of the respective Arabidopsis ecotype; comparative analyses of wild type Wassilewskija (Ws) carrying an independent loss-of-function allele of *GORK* (Hosy et al., 2003) revealed similar results (Fig. 2E). Together, these results establish GORK $K^+$ efflux channel function as an essential step during the JA-induced stomatal closure process.

**GORK specifically associates with the CBL-interacting kinase CIPK5 and the PP2C-type phosphatase ABI2**

ABA and JA have been reported to trigger $Ca^{2+}$-oscillations in guard cells (Islam et al., 2010; Allen et al., 2001). To identify $Ca^{2+}$-regulated kinases that potentially could modulate GORK activity, we performed yeast two-hybrid analyses of guard cell-expressed members of the

calcineurin B-like interacting protein kinase family (Fig. S4A) together with the cytoplasmic N-terminal domain (NT) of the GORK channel. Only co-expression of CIPK5 with GORK-NT resulted in significantly enhanced ß-galactosidase reporter activity, suggesting a specific interaction of GORK-NT with this kinase (Fig. 3A). We next combined CIPK5 with all 10 CBLs from Arabidopsis, detecting strong interaction between CIPK5 and the $Ca^{2+}$ sensors CBL1, CBL4, CBL5 and CBL9 (Fig. S4B). To further analyze these potential interactions *in planta*, we employed bimolecular fluorescence complementation (BiFC) assays in transiently transformed *N. benthamiana* leaves (Waadt and Kudla, 2008). Co-expression of full-length GORK (GORK-$YFP^C$) with CIPK5 ($YFP^N$-CIPK5) resulted in readily detectable fluorescence, indicating efficient interaction between both proteins (Fig. 3B, left). In contrast, co-expression of GORK with the guard cell expressed kinase CIPK15 ($YFP^N$-CIPK15; Fig. 3B, right) did not result in detectable fluorescence above background levels implying specificity of the observed CIPK5-GORK interaction. Efficient interaction of CIPK5 with GORK was also observed in BiFC analyses of transiently transfected Arabidopsis protoplasts (Fig. 3C, left panel). To identify which of the guard cell CBLs provide for plasma membrane localization of their interacting CIPKs (Batistic et al., 2010), we focused initially on the guard cell-expressed $Ca^{2+}$ sensors CBL1 and CBL9 (see Fig. S5), incorporating CBL7 as a potential negative control (Fig. S4B). These analyses revealed an efficient interaction of CIPK5 with CBL1 and CBL9 at the plasma membrane, but not with CBL7 (Fig. 3D). Membrane-targeting of CIPKs in plant cells depends on their interaction with specific CBL proteins and previous studies have revealed that co-expression of CBL proteins can also affect the subcellular trafficking of for example AKT2 $K^+$ channels (Batistic et al., 2010; Held et al., 2011). We therefore performed interaction analyses

of GORK and CIPK5 in the presence or absence of either full-length (CBL1-OFP) or truncated (CBL1n-OFP) CBL1 protein (Fig. 3E) in transiently transformed tobacco leaves. In the presence of CBL1n-OFP, we observed interaction of the kinase with the $K^+$ channel at the plasma membrane but also in punctuate cellular structures implying that a significant percentage of the CIPK5-GORK complexes accumulated at the endoplasmic reticulum. This was particularly evident around the nucleus (see Fig. 3E, lower panel). Upon co-expression of the full-length plasma membrane-localized CBL1-OFP, CIPK5-GORK localization pattern changed dramatically (Fig. 3E, upper panel). The kinase- $K^+$ channel complexes were efficiently translocated to the plasma membrane. Sole expression of the C-terminal truncated version of CBL1 (CBL1n-OFP) harboring the N-terminally located dual fatty acyl modification motif (Batistic et al., 2008), resulted in efficient plasma membrane targeting of the $Ca^{2+}$ sensor protein (Fig. 3E; right panel). Impaired in its functional interaction with the CIPK5 protein, however, the truncated CBL1 version failed to provide for proper plasma membrane targeting of the GORK channel. Together, these data establish the efficient interaction of the kinase CIPK5 with the $K^+$ channel GORK in plant cells and suggest a positive impact of CBL1 on CIPK5-GORK interaction at the plasma membrane.

To identify regulatory components counteracting the potential impact of CBL1-CIPK5 on GORK, we extended our analyses towards the guard cell expressed PP2C-type protein phosphatases ABI1 and ABI2, both well-known negative regulators of ABA-dependent stomatal closure (Cutler et al., 2010; Rubio et al., 2009). We did not obtain evidence of an interaction of ABI1 with the GORK N-terminal domain in yeast two-hybrid analyses. However,

upon co-expression of GORK-NT with the PP2C ABI2 we clearly observed reporter gene activation, which is indicative of a protein-protein interaction (see Fig. 3A). Additional BiFC analyses in *Arabidopsis* mesophyll protoplasts provided further support for an interaction of ABI2 with GORK, as well as with CIPK5 *in planta* (Fig. 3C). Taken together, our results indicate that the N-terminus of GORK conveys interaction with the ABA-inactivated phosphatase ABI2 and with $Ca^{2+}$-activated CBL1-CIPK5 complexes. This allows for potentially antagonistic regulation of the $K^+$ channel by these signaling components via a phosphorylation/ dephosphorylation switch.

**The N-terminal domain of GORK is phosphorylated by CIPK5 and de-phosphorylated by ABI2**

To biochemically investigate a potential regulatory phosphorylation-dephosphorylation mechanism for GORK, we performed phosphorylation experiments *in vitro* using recombinant proteins. Combining GORK N-terminal and C-terminal cytoplasmic domains with CIPK5 in *in vitro* phosphorylation experiments revealed that this kinase only phosphorylated the GORK amino terminus (Fig. 4A). Consistent with its role as a suppressor of channel activity, CIPK5 dependent phosphorylation of the GORK N-terminus was suppressed when ABI2 was present (Fig. 4B; lane 5). This inhibitory effect of ABI2 was also apparent when the phosphatase was added 30 min after the start of the kinase reaction (Fig. 4B, lane 6). This suggests that ABI2 is not only capable of interacting with CIPK5 and GORK (see Fig. 3A and C), but also dephosphorylates the N-terminus of the guard cell channel $K^+$ efflux channel. Compared to e.g. CIPK1 or CIPK23 autophosphorylation activity of CIPK5 was low (Fig. S5B, lanes 1 – 3) and was not enhanced in the presence of CBL1 (Fig. S5B, lanes 4 – 6). Likewise, the efficacy of

CIPK5 to phosphorylate the GORK N-terminus was unabatedly high irrespective of absence or presence of CBL1 (Fig. S5B, lanes 8 and 9).

**Antagonistic regulation of guard cell $K^+$ efflux channel GORK by ABI2 and CBL1/9-CIPK5**

To analyze the functional consequences of the protein-protein interaction between GORK and the protein phosphatase ABI2, as well as with the CBL1/9-CIPK5 $Ca^{2+}$ sensor-kinase complexes, we characterized channel regulation in the heterologous *Xenopus* oocyte expression system using the two-electrode voltage clamp (TEVC) technique. Upon co-expression of the PP2C ABI2, GORK steady-state currents were reduced by 74.0±1.9%, to 26.0±1.9% of the original currents, indicating that the ABI2 phosphatase represents a negative regulator of the guard cell $K^+_{out}$ channel (Fig. 5A-C). In contrast to ABI2 and in line with the yeast two-hybrid studies, GORK currents remained unaffected in the presence of ABI1 ($I_{SS}$ = 88.1±8.6%, Fig. 5C). We then explored a possible function for the CBL1/9-CIPK5 $Ca^{2+}$ sensor-kinase complexes in GORK regulation, co-expressing the GORK channel together with ABI2, and CIPK5 with either CBL1 or CBL9 (Fig. 5). These experiments revealed that ABI2-mediated inhibition of GORK activity was similarly relieved by CBL1-CIPK5 and by CBL9-CIPK5 complexes. Co-expression of CBL1-CIPK5 or CBL9-CIPK5 counteracted the ABI2 inhibition, restoring respectively, 55.8±4.3% and 56.6±4.2% of the maximum GORK channel activity (Fig. 5D). Activation of GORK was specifically dependent on CIPK5; replacement of CIPK5 by CIPK15 did not affect ABI2 inhibition of GORK currents (31.3±3.2%, Fig. 5D). Importantly, release of ABI2-mediated inhibition of GORK activity required CIPK5 kinase activity. Mutated versions of CIPK5 exhibiting either a mutation in the ATP binding site ($CIPK5^{K41N}$; Maierhofer et al., 2014) or in the activation loop

(CIPK5$^{D153N}$) were inefficient in restoring GORK activity as compared to wild type CIPK5 (Fig. 5E). Measurements of GORK activity upon co-expression of CIPK5$^{K41N}$ or CIPK5$^{D153N}$ revealed 19.6±3.2% and 20.3±3.3% of maximal channel activity, respectively.

As expected, in the absence of CBL proteins the CIPK5 kinase on its own did not relieve ABI2-mediated inhibition of GORK channel activity (Fig. 5D; 27.6±4.9%), again demonstrating a pivotal role of CBL calcium sensors for $Ca^{2+}$ sensor-kinase complex activity towards their substrates (Leran et al., 2015; Hashimoto et al., 2012; Xu et al., 2006). When compared to wt-CBL1, expression of CBL1$^{G2A}$, a mutant disrupted in plasma membrane anchoring, severely impaired the CIPK5-mediated activation of GORK (Fig. 5E; 24.7±2.7%).

We next investigated whether $Ca^{2+}$ binding to the CBL1 protein conveys the $Ca^{2+}$-dependent regulation of GORK activity by mutating $Ca^{2+}$-coordinating amino acids in the $Ca^{2+}$-binding EF-hands of CBL1. TEVC recordings in *Xenopus* oocytes revealed that the GORK-mediated $K^+$ currents were significantly reduced to 32.1±4.8 % of the non-mutated CBL1 protein when co-expressed with CIPK5 and CBL1$^{E172Q}$, which harbors a single site mutation on the fourth EF-hand (Fig. 5E). When all four EF-hands of CBL1 were mutated (CBL1$^{E56Q\ D91N\ E128Q\ E172Q}$), the GORK-mediated $K^+$ currents were further reduced to 19.0±3.1 % compared to CBL1-induced values (Fig. 5E). Together with the interaction/localization studies (see Fig. 3E) these results establish that plasma membrane-targeting of CBL1 by lipid-modification of its N-terminus is essential for activation of GORK by CBL1-CIPK5 complexes. Moreover, these data imply that $Ca^{2+}$ binding to CBL1 represents an important step in translating a JA-induced $Ca^{2+}$ signal into $K^+$ efflux channel activation.

**JA-signaling requires a CBL1/9-CIPK5 $Ca^{2+}$ sensor/kinase complex as a positive regulator of JA triggered stomatal closure**

So far, our results suggested that JA-signaling activates a CBL1/9-CIPK5 $Ca^{2+}$ relay that promotes GORK mediated $K^+$ efflux in guard cells. To address this hypothesis, we extended our patch-clamp recordings towards guard cell protoplasts of the *cipk5-2* kinase loss-of-function mutant (Fig. S6A and B). As expected, guard cell protoplasts of the *cipk5-2* mutant exhibited outward and inward $K^+$ currents comparable to wt (see Fig. 2A and C) under control conditions (Fig. 6A). Comparable to wt and *gork1-2* (see Fig. 2A-C) COR inhibited $K_{in}$ current activity in the kinase mutant (Fig. 6B and C). In contrast to wt however, the JA-mimic failed to stimulate $K^+_{out}$ activity. Therefore, in line with phosphorylation studies and two-electrode-voltage-clamp recordings our patch clamp data suggested an important role for CIPK5 in JA-triggered fast stomatal closure. We therefore employed a genetic approach to unravel the physiological function of CBL1/9-CIPK5 as well as ABI2 in JA-triggered guard cell regulation. We isolated and comparatively analyzed respective loss-of-function mutants of the identified channel regulators for their capability to respond to the closure stimuli ABA and MeJA. Incubation of intact leaves of 5 to 6-week-old Arabidopsis wild type plants with either 20 µM (±)-ABA or 10 µM MeJA caused stomatal closure within 30-60 min (data not shown). After 1 h, guard cells of the *cipk5-2* mutant and the *cbl1/9* double mutant were fully closed in response to ABA, resembling wt-like responsiveness in this respect (Fig. 6D). In contrast to wild type, but reminiscent of the *gork* mutants (Fig. 2D and E), guard cells of neither mutant closed in response to exogenously-applied MeJA (Fig. 6D, and Fig. S6C). Similar to *cipk5-2*, an

independent *CIPK5* loss-of-function allele (*cipk5-1*) did not exhibit impaired ABA responses, but instead displayed strongly reduced responses to MeJA application (Fig. S6C). Importantly, complementation of both *cipk5* mutant alleles with a genomic fragment encompassing the *CIPK5* gene restored the response to JA (Fig. S6D). We further observed that the *cbl9* single mutant exhibited partial insensitivity to MeJA (Fig. S6E), while both *cbl1* and the *cbl1/cbl9* double mutant were incapable of transducing the MeJA signal into a stomatal closure response (Fig. 6D and S6E). These results identify CBL-type $Ca^{2+}$ sensor proteins and their interacting kinase as essential components in fast JA signal transduction. Moreover, these data provide strong evidence that CBL1/9-CIPK5 complexes are essential for JA-triggered guard cell closure via their activating role for the GORK $K^+$ efflux channel. In order to assess the role of PP2Cs in guard cell jasmonate signaling, we also tested the ABA insensitive *abi1-1* and *abi2-1* mutant alleles, which both express mutant phosphatases refractory to inhibition by ABA receptors, in stomata aperture assays (Fig. 6D). In line with their reduced ABA sensitivity, stomata of both mutant lines exhibited greater apertures under control conditions (0.54±0.01 and 0.47±0.01, respectively; Ler WT: 0.41±0.01) and guard cell closing responses to ABA appeared attenuated when compared to wild type plants (0.38±0.01 and 0.32±0.01; Ler WT: 0.29±0.01). In contrast to *abi1-1,* which responded similarly to ABA and MeJA, stomata of *abi2-1* did not close in response to JA application (0.39±0.01 and 0.47±0.01; Ler WT: 0.21±0.01). These data further corroborate the conclusion that ABI2 but not ABI1 represents a component of JA-induced signaling processes that regulate GORK activity and guard cell aperture (Fig. S6F). Moreover, these data suggest that, with respect to JA-induced stomatal closure, ABI2 function appears to be distinct from its role in ABA signaling.

Considering that JA-induced stomatal closure specifically involves ABI2, a key regulator of ABA perception and signaling, it is well conceivable that JA signaling in guard cells involves ABA-biosynthesis, -signaling or both. JA induced stomatal closure requires the functional JA receptor since guard cells of the jasmonate receptor mutant *CORONATINE INSENSITIVE 1 (coi1-16)* remained open in response to jasmonate but displayed normal susceptibility towards ABA (Fig. S7A). On the other hand, we observed only a marginal effect of JA on ABA biosynthesis. Guard cells of the ABA-reporting ABAleon2 plants (Waadt, et al., 2014) showed markedly increased cytosolic ABA levels upon ABA treatment, but only moderate signs of elevated ABA levels 1 h following MeJA application (Fig. S7B). Mutations targeting key players of ABA induced stomatal closure, such as the sugar-non-fermenting kinase SnRK2.6 (OST1) or the guard cell S-type anion channel SLAC1 appeared insensitive to JA (Fig. S7A), suggesting that the wounding hormone JA recruits specific elements of the guard cell ABA signaling cascade, including the GORK $K^+$ efflux channel. In a physiological context this hypothesis is substantiated by the observation that comparable to JA treatment stomatal closure in the *gork* mutant in response to wounding is impaired locally as well as systemically (Fig. 6E).

## Discussion

### GORK-dependent $K^+$ efflux is specifically required for wound-induced, JA-controlled stomatal closure

Our identification of GORK as the $K^+$ efflux channel essential for wound-induced, JA-controlled but not for flg22 or ABA-induced guard cell closure, uncovers unexpected and important differences in the contribution of $K^+$ channels to guard cell function. It also points towards fundamental differences in the operational mode of the two hormones (Osakabe et al., 2013). JA action in guard cells is fast and precedes wound induced stomatal closure (see **Fig. 1**). Our observation that the GORK channel is activated already 15 minutes following JA application (see Fig. 2) is in further support of a fast-signaling chain. However, JA induced stomatal closure requires both functional JA and ABA receptors. Guard cells of the *coi1-16* as well as the *pyr/pyl1245* mutants remained open in response to wounding or jasmonate (Fig. S7A). JA-induced stomatal closure specifically involves the ABA coreceptor ABI2 and in addition the sugar-non-fermenting kinase SnRK2.6 (OST1) and the guard cell S-type anion channel SLAC1 (Fig. S7A). This genetic evidence is in line with recent findings by Yin et al. (2016) proposing that the wounding hormone may JA recruit specific elements of the guard cell ABA signaling cascade. Further, oxylipins and ABA together seem to control stomatal conductance in response to wounding and herbivore oral secretions, resulting decreased photosynthetic carbon assimilation in *Nicotiana attenuata* (Meza-Canales et al., 2017). Further, *Brassica napus* guard cell metabolomics has recently shown that high $CO_2$-induced stomatal closure is mediated by JA-Ile and JA signaling, too (Geng et al., 2016); interestingly, without affecting guard cell ABA levels. This might suggest that fast JA signaling impinges on guard cell ABA sensitivity rather than ABA biosynthesis.

**$Ca^{2+}$-dependent phosphorylation is essential for activation of GORK-mediated $K^+$ efflux in guard cells**

Both ABA and JA trigger $Ca^{2+}$ signals in guard cells (Islam et al., 2010; Allen et al., 2001), possibly via the cyclic nucleotide gated channel CNGC2 (Lu et al., 2016). This work identifies a previously unknown $Ca^{2+}$-signaling module that specifically functions in JA signaling. Specifically, our studies revealed the guard cell $K^+$-efflux GORK in *Arabidopsis* as a target of CBL1/9-CIPK5 $Ca^{2+}$ sensor/kinase complexes. Based on our interaction and phosphorylation studies, we conclude that the association of the CBL1/9-CIPK5 module with GORK at the plasma membrane leads to channel phosphorylation at its cytosolic N- terminal domain. Our results further imply that GORK phosphorylation in turn promotes channel activation, hence $K^+$ efflux from guard cells. This type of regulation is reminiscent of the mechanism of activation of the guard cell anion channels SLAC1 and SLAH3 (SLAC1 HOMOLOG 3) during ABA-mediated stomatal closure by members of the CPK family and CBL1/9-CIPK23 (Maierhofer et al., 2014; Brandt et al., 2012; Scherzer et al., 2012; Geiger et al., 2010).

A noteworthy observation from our studies is that, similar to *gork* mutants, loss-of-function of the single $Ca^{2+}$ sensor CBL1 or its interacting kinase CIPK5 completely abolishes the JA-response in guard cells. Not only does this establish a unique and essential role for CBL1-CIPK5 complexes in JA-signaling, but it also raises important questions about the functional specificity of CBL-CIPK complexes in general. Both the $Ca^{2+}$ sensors CBL1 and CBL9 have been shown to accomplish important functions in various processes such as root $K^+$ uptake, guard cell drought stress responses and nitrate sensing by interacting with the kinase CIPK23 and

phosphorylating the $K^+$ influx channel AKT1 or the nitrate transporter NPF6.3 (Leran et al., 2015; Cheong et al., 2007; Xu et al., 2006). However, in contrast to their function in JA-mediated stomatal closing single CBL1 or CBL9 mutants did not impinge on nitrate or potassium sensing and it required the analyses of *cbl1/cbl9* double mutants to observe discernable phenotypes. This points towards functional specificity of distinct CBL1-CIPK complexes during JA, ABA and low nitrate or $K^+$-related signaling processes.

**The role of PP2C-type phosphatases in fast, JA-mediated stomatal closure**

Phosphorylation-dependent SLAC/SLAH anion activation is counteracted by several PP2C-type phosphatases including PP2CA, ABI1 and ABI2 (Geiger et al., 2009; Lee et al., 2009). We observed that CBL1/9-CIPK5 dependent activation of GORK was specifically antagonized by ABI2, but not by ABI1, thus establishing a distinct role of ABI2 for JA signaling. Employing CIPK5 in phosphorylation assays further revealed that ABI2 is capable of dephosphorylating GORK (Fig. 4B). Together with our functional studies on GORK activity, we thus conclude that ABI2 antagonizes CIPK5 action and acts as a negative regulator of GORK-mediated $K^+$ efflux in guard cells. However, we cannot exclude the possibility that, in addition to direct dephosphorylation of GORK, ABI2 also directly inhibits the activity of CIPK5. Such PP2C-mediated mechanism of dual inhibition of a CIPK and its substrate has recently been reported for SLAC1 (Maierhofer et al., 2014). Nevertheless, such a scenario would not affect the general conclusion that ABI2 represents a negative regulator of GORK activity (see Fig. 5 and Lefoulon et al., 2016).

Based on the data reported here and considering the available published evidence, we propose the following model of JA function in regulating guard cell closure (Fig. 7). Stimulus-

induced elevations of guard cell JA concentrations activate JA signaling via COI1 receptors (see Fig S7A). JA triggers $Ca^{2+}$ signatures (Lu et al., 2016; Murata et al., 2015) and activates ABA signaling, which is in line with the requirement of functional ABA receptors for JA-induced stomatal closure reactions (Fig. S7 and Yin et al., 2016). ABA signaling inactivates ABI2, thereby releasing the inhibition of GORK activity. In parallel, the increase in cytosolic $Ca^{2+}$ concentration triggers $Ca^{2+}$-dependent phosphorylation of guard cell anion channels leading to membrane potential depolarization. This depolarization is pivotal for activation of the voltage-dependent outward-rectifying $K^+$ channel GORK. Of equal importance, increasing cytosolic $Ca^{2+}$ concentrations favor CBL1/9-CIPK5 mediated GORK channel phosphorylation, a further pre-requisite for channel activation. Together, plasma membrane depolarization and phosphorylation synergistically promote potassium efflux. In this manner, convergence of hormone and $Ca^{2+}$-mediated activation allows for efficient fine-tuning of GORK-mediated $K^+$ efflux for tightly regulating stomatal aperture adjustment and provides the mechanistic flexibility to facilitate stomatal closure in response to diverse stimuli such as drought and light stress (Devireddy et al., 2018) or wounding.

**Acknowledgements**

The authors would like to thank Stefanie Schültke and Linda Beckmann for their contribution of early interaction studies, and Jan Niklas Offenborn for providing reagents and constructs. We thank Rainer Hedrich, Tracey Ann Cuin, Elzbieta Król and Dietmar Geiger for helpful

discussions and critical comments to the manuscript and Irene Marten for supporting the patch clamp experiments. This work was supported by grants from the Deutsche Forschungsgemeinschaft (DFG) within the GK1342 “lipid signaling” to D.B., and within the DFG research group FOR964 to D.B., E.G. and J.K.

**Author Contributions**

D.B., J.K. and E.G. conceived the project. D.B. supervised the project. P.L.R., E.G., J.K. and D.B. designed all experiments; S.F., U.A. and E.K. characterized guard cell phenotypes. A.L. performed stoma assays in combination with JA signaling studies in guard cells. U.A. and L.K. did the yeast two-hybrid interaction studies. S.H. performed wounding induced guard cell imaging studies. S.F. and R.W. monitored *in situ* guard cell ABA changes. S.F. and U.A. performed two-electrode voltage clamp studies. E.K. conducted patch-clamp experiments. L.K.S., P.K. and K.S. performed in vitro phosphorylation studies. O.B., P.K. and. S.F. performed microscopy and interaction studies. S.F., E.K., J.K. and D.B. wrote the paper.

**Declaration of Interests**

The authors declare that they have no competing interests.

**References**

Ache, P., Becker, D., Ivashikina, N., Dietrich, P., Roelfsema, M.R., and Hedrich, R. (2000). GORK, a delayed outward rectifier expressed in guard cells of *Arabidopsis thaliana*, is a $K^+$-selective, $K^+$-sensing ion channel. FEBS Lett. 486, 93-8.

Albrecht, V., Ritz, O., Linder, S., Harter, K., and Kudla, J. (2001). The NAF domain defines a novel protein-protein interaction module conserved in $Ca^{2+}$-regulated kinases. EMBO J. 20, 1051-63.

Allen, G.J., Chu, S.P., Harrington, C.L., Schumacher, K., Hoffmann, T., Tang, Y.Y., Grill, E., and Schroeder, J.I. (2001). A defined range of guard cell calcium oscillation parameters encodes stomatal movements. Nature 411, 1053-7.

Anschütz, U., Becker, D., and Shabala, S. (2014). Going beyond nutrition: Regulation of potassium homoeostasis as a common denominator of plant adaptive responses to environment. J. Plant Physiol. 171, 670-687.

Batistic, O., Sorek, N., Schultke, S., Yalovsky, S., and Kudla, J. (2008). Dual fatty acyl modification determines the localization and plasma membrane targeting of CBL/CIPK $Ca^{2+}$ signaling complexes in Arabidopsis. Plant Cell 20, 1346-62.

Batistic, O., Waadt, R., Steinhorst, L., Held, K., and Kudla, J. (2010). CBL-mediated targeting of CIPKs facilitates the decoding of calcium signals emanating from distinct cellular stores. Plant J. 61, 211-22.

Bauer, H., Ache, P., Lautner, S., Fromm, J., Hartung, W., Al-Rasheid, K.A., Sonnewald, S., Sonnewald, U., Kneitz, S., Lachmann, N., et al. (2013). The Stomatal Response to Reduced Relative Humidity Requires Guard Cell-Autonomous ABA Synthesis. Current biology : CB 23, 53-7.

Brandt, B., Brodsky, D.E., Xue, S., Negi, J., Iba, K., Kangasjarvi, J., Ghassemian, M., Stephan, A.B., Hu, H., and Schroeder, J.I. (2012). Reconstitution of abscisic acid activation of SLAC1 anion channel by CPK6 and OST1 kinases and branched ABI1 PP2C phosphatase action. Proc Natl Acad Sci U S A 109, 10593-8.

Cheong, Y.H., Pandey, G.K., Grant, J.J., Batistic, O., Li, L., Kim, B.G., Lee, S.C., Kudla, J., and Luan, S. (2007). Two calcineurin B-like calcium sensors, interacting with protein kinase CIPK23, regulate leaf transpiration and root potassium uptake in Arabidopsis. Plant J. 52, 223-39.

Corratge-Faillie, C., Ronzier, E., Sanchez, F., Prado, K., Kim, J.H., Lanciano, S., Leonhardt, N., Lacombe, B., and Xiong, T.C. (2017). The Arabidopsis guard cell outward potassium channel GORK is regulated by CPK33. FEBS Lett 591, 1982-1992.

Cutler, S.R., Rodriguez, P.L., Finkelstein, R.R., and Abrams, S.R. (2010). Abscisic acid: emergence of a core signaling network. Annu. Rev. Plant Biol. 61, 651-79.

Devireddy, A.R., Zandalinas, S.I., Gómez-Cadenas, A., Blumwald, E., and Mittler, R. (2018). Coordinating the overall stomatal response of plants: Rapid leaf-to-leaf communication during light stress. Science Signaling 11.

Drerup, M.M., Schlucking, K., Hashimoto, K., Manishankar, P., Steinhorst, L., Kuchitsu, K., and Kudla, J. (2013). The Calcineurin B-like calcium sensors CBL1 and CBL9 together with their interacting protein kinase CIPK26 regulate the Arabidopsis NADPH oxidase RBOHF. Mol Plant 6, 559-69.

Evans, N.H. (2003). Modulation of guard cell plasma membrane potassium currents by methyl jasmonate. Plant Physiol. 131, 8-11.

Felix, G., Duran, J.D., Volko, S., and Boller, T. (1999). Plants have a sensitive perception system for the most conserved domain of bacterial flagellin. Plant J. 18, 265-76.

Geiger, D., Scherzer, S., Mumm, P., Marten, I., Ache, P., Matschi, S., Liese, A., Wellmann, C., Al-Rasheid, K.A., Grill, E., et al. (2010). Guard cell anion channel SLAC1 is regulated by CDPK protein kinases with distinct $Ca^{2+}$ affinities. Proc Natl Acad Sci U S A 107, 8023-8.

Geiger, D., Scherzer, S., Mumm, P., Stange, A., Marten, I., Bauer, H., Ache, P., Matschi, S., Liese, A., Al-Rasheid, K.A., et al. (2009). Activity of guard cell anion channel SLAC1 is controlled by drought-stress signaling kinase-phosphatase pair. Proc Natl Acad Sci U S A 106, 21425-30.

Geng, S., Misra, B.B., de Armas, E., Huhman, D.V., Alborn, H.T., Sumner, L.W., and Chen, S. (2016). Jasmonate-mediated stomatal closure under elevated CO2 revealed by time-resolved metabolomics. Plant J 88, 947-962.

Gfeller, A., Liechti, R., and Farmer, E.E. (2010). Arabidopsis jasmonate signaling pathway. Sci Signal 3, cm4.

Glazebrook, J. (2005). Contrasting mechanisms of defense against biotrophic and necrotrophic pathogens. Annu Rev Phytopathol 43, 205-27.

Hashimoto, K., Eckert, C., Anschutz, U., Scholz, M., Held, K., Waadt, R., Reyer, A., Hippler, M., Becker, D., and Kudla, J. (2012). Phosphorylation of calcineurin B-like (CBL) calcium sensor proteins by their CBL-interacting protein kinases (CIPKs) is required for full activity of CBL-CIPK complexes toward their target proteins. J. Biol. Chem. 287, 7956-68.

Hashimoto, K., and Kudla, J. (2011). Calcium decoding mechanisms in plants. Biochemie 93, 2054-9.

Hedrich, R. (2012). Ion channels in plants. Physiol. Rev. 92, 1777-811.

Hedrich, R., and Geiger, D. (2017). Biology of SLAC1-type anion channels - from nutrient uptake to stomatal closure. New Phytol. 216, 46-61.

Held, K., Pascaud, F., Eckert, C., Gajdanowicz, P., Hashimoto, K., Corratge-Faillie, C., Offenborn, J.N., Lacombe, B., Dreyer, I., Thibaud, J.B., et al. (2011). Calcium-dependent modulation and

plasma membrane targeting of the AKT2 potassium channel by the CBL4/CIPK6 calcium sensor/protein kinase complex. Cell Res. 21, 1116-30.

Hetherington, A.M. (2001). Guard Cell Signaling. Cell 107, 711-714.

Himmelbach, A., Hoffmann, T., Leube, M., Hohener, B., and Grill, E. (2002). Homeodomain protein ATHB6 is a target of the protein phosphatase ABI1 and regulates hormone responses in Arabidopsis. EMBO J. 21, 3029-38.

Hosy, E., Vavasseur, A., Mouline, K., Dreyer, I., Gaymard, F., Poree, F., Boucherez, J., Lebaudy, A., Bouchez, D., Very, A.A., et al. (2003). The Arabidopsis outward $K^+$ channel GORK is involved in regulation of stomatal movements and plant transpiration. Proc Natl Acad Sci U S A 100, 5549-54.

Imes, D., Mumm, P., Bohm, J., Al-Rasheid, K.A., Marten, I., Geiger, D., and Hedrich, R. (2013). Open stomata 1 (OST1) kinase controls R-type anion channel QUAC1 in Arabidopsis guard cells. Plant J. 74, 372-82.

Islam, M.M., Hossain, M.A., Jannat, R., Munemasa, S., Nakamura, Y., Mori, I.C., and Murata, Y. (2010). Cytosolic alkalization and cytosolic calcium oscillation in Arabidopsis guard cells response to ABA and MeJA. Plant Cell Physiol. 51, 1721-30.

Larrieu, A., Champion, A., Legrand, J., Lavenus, J., Mast, D., Brunoud, G., Oh, J., Guyomarc'h, S., Pizot, M., Farmer, E.E., et al. (2015). A fluorescent hormone biosensor reveals the dynamics of jasmonate signalling in plants. Nat Commun 6, 6043.

Lee, S.C., Lan, W., Buchanan, B.B., and Luan, S. (2009). A protein kinase-phosphatase pair interacts with an ion channel to regulate ABA signaling in plant guard cells. Proc Natl Acad Sci U S A 106, 21419-24.

Lefoulon, C., Boeglin, M., Moreau, B., Very, A.A., Szponarski, W., Dauzat, M., Michard, E., Gaillard, I., and Cherel, I. (2016). The Arabidopsis AtPP2CA Protein Phosphatase Inhibits the GORK $K^+$ Efflux Channel and Exerts a Dominant Suppressive Effect on Phosphomimetic-activating Mutations. J. Biol. Chem. 291, 6521-33.

Leran, S., Edel, K.H., Pervent, M., Hashimoto, K., Corratge-Faillie, C., Offenborn, J.N., Tillard, P., Gojon, A., Kudla, J., and Lacombe, B. (2015). Nitrate sensing and uptake in Arabidopsis are enhanced by ABI2, a phosphatase inactivated by the stress hormone abscisic acid. Sci Signal 8, ra43.

Lu, M., Zhang, Y., Tang, S., Pan, J., Yu, Y., Han, J., Li, Y., Du, X., Nan, Z., and Sun, Q. (2016). AtCNGC2 is involved in jasmonic acid-induced calcium mobilization. J. Exp. Bot. 67, 809-19.

Kolukisaoglu, U., Weinl, S., Blazevic, D., Batistic, O., and Kudla, J. (2004). Calcium sensors and their interacting protein kinases: genomics of the Arabidopsis and rice CBL-CIPK signaling networks. Plant Physiol. 134, 43-58.

Maierhofer, T., Diekmann, M., Offenborn, J.N., Lind, C., Bauer, H., Hashimoto, K., KA, S.A.-R., Luan, S., Kudla, J., Geiger, D., et al. (2014). Site- and kinase-specific phosphorylation-mediated activation of SLAC1, a guard cell anion channel stimulated by abscisic acid. Sci Signal 7, ra86.

McLachlan, D.H., Kopischke, M., and Robatzek, S. (2014). Gate control: guard cell regulation by microbial stress. New Phytol. 203, 1049-1063.

Melotto, M., Underwood, W., and He, S.Y. (2008). Role of stomata in plant innate immunity and foliar bacterial diseases. Annu. Rev. Phytopathol. 46, 101-22.

Meza-Canales, I.D., Meldau, S., Zavala, J.A., and Baldwin, I.T. (2017). Herbivore perception decreases photosynthetic carbon assimilation and reduces stomatal conductance by engaging 12-oxo-phytodienoic acid, mitogen-activated protein kinase 4 and cytokinin perception. Plant, cell & environment 40, 1039-1056.

Montillet, J.L., and Hirt, H. (2013). New checkpoints in stomatal defense. Trends Plant Sci. 18, 295-7.

Mousavi, S.A., Chauvin, A., Pascaud, F., Kellenberger, S., and Farmer, E.E. (2013). GLUTAMATE RECEPTOR-LIKE genes mediate leaf-to-leaf wound signalling. Nature 500, 422-6.

Murata, Y., Mori, I.C., and Munemasa, S. (2015). Diverse stomatal signaling and the signal integration mechanism. Annu. Rev. Plant Biol. 66, 369-92.

Nabity, P.D., Zavala, J.A., and DeLucia, E.H. (2013). Herbivore induction of jasmonic acid and chemical defences reduce photosynthesis in Nicotiana attenuata. J Exp Bot 64, 685-94.

Nour-Eldin, H.H., Norholm, M.H., and Halkier, B.A. (2006). Screening for plant transporter function by expressing a normalized Arabidopsis full-length cDNA library in Xenopus oocytes. Plant Methods 2, 17.

Osakabe, Y., Arinaga, N., Umezawa, T., Katsura, S., Nagamachi, K., Tanaka, H., Ohiraki, H., Yamada, K., Seo, S.U., Abo, M., et al. (2013). Osmotic stress responses and plant growth controlled by potassium transporters in Arabidopsis. Plant Cell 25, 609-24.

Raghavendra, A.S., Gonugunta, V.K., Christmann, A., and Grill, E. (2010). ABA perception and signalling. Trends Plant Sci. 15, 395-401.

Roelfsema, M.R., and Hedrich, R. (2005). In the light of stomatal opening: new insights into 'the Watergate'. New Phytol 167, 665-91.

Rubio, S., Rodrigues, A., Saez, A., Dizon, M.B., Galle, A., Kim, T.H., Santiago, J., Flexas, J., Schroeder, J.I., and Rodriguez, P.L. (2009). Triple loss of function of protein phosphatases type 2C leads to partial constitutive response to endogenous abscisic acid. Plant Physiol. 150, 1345-55.

Savchenko, T., Kolla, V.A., Wang, C.-Q., Nasafi, Z., Hicks, D.R., Phadungchob, B., Chehab, W.E., Brandizzi, F., Froehlich, J., and Dehesh, K. (2014). Functional Convergence of Oxylipin and Abscisic Acid Pathways Controls Stomatal Closure in Response to Drought. Plant Physiol. 164, 1151-1160.

Sawinski, K., Mersmann, S., Robatzek, S., and Bohmer, M. (2013). Guarding the green: Pathways to stomatal immunity. Mol Plant Microbe Interact 26, 626-32.

Scherzer, S., Maierhofer, T., Al-Rasheid, K.A., Geiger, D., and Hedrich, R. (2012). Multiple Calcium-Dependent Kinases Modulate ABA-Activated Guard Cell Anion Channels. Molecular plant 5, 1409-12.

Schindelin, J., Arganda-Carreras, I., Frise, E., Kaynig, V., Longair, M., Pietzsch, T., Preibisch, S., Rueden, C., Saalfeld, S., Schmid, B., et al. (2012). Fiji: an open-source platform for biological-image analysis. Nat Meth 9, 676-682.

Schroeder, J.I., Allen, G.J., Hugouvieux, V., Kwak, J.M., and Waner, D. (2001). Guard cell signal transduction. Annu. Rev. Plant Physiol. Plant Mol. Biol. 52, 627-658.

Sheard, L.B., Tan, X., Mao, H., Withers, J., Ben-Nissan, G., Hinds, T.R., Kobayashi, Y., Hsu, F.-F., Sharon, M., Browse, J., et al. (2010). Jasmonate perception by inositol-phosphate-potentiated COI1–JAZ co-receptor. Nature 468, 400.

Vahisalu, T., Kollist, H., Wang, Y.F., Nishimura, N., Chan, W.Y., Valerio, G., Lamminmaki, A., Brosche, M., Moldau, H., Desikan, R., et al. (2008). SLAC1 is required for plant guard cell S-type anion channel function in stomatal signalling. Nature 452, 487-91.

Waadt, R., Hitomi, K., Nishimura, N., Hitomi, C., Adams, S.R., Getzoff, E.D., and Schroeder, J.I. (2014). FRET-based reporters for the direct visualization of abscisic acid concentration changes and distribution in Arabidopsis. http://dx.doi.org/10.7554/eLife.01739.001.

Waadt, R., and Kudla, J. (2008). In Planta Visualization of Protein Interactions Using Bimolecular Fluorescence Complementation (BiFC). CSH Protoc 2008, pdb prot4995.

Xie, D.X., Feys, B.F., James, S., Nieto-Rostro, M., and Turner, J.G. (1998). COI1: an Arabidopsis gene required for jasmonate-regulated defense and fertility. Science 280, 1091-4.

Xu, J., Li, H.D., Chen, L.Q., Wang, Y., Liu, L.L., He, L., and Wu, W.H. (2006). A protein kinase, interacting with two calcineurin B-like proteins, regulates $K^+$ transporter AKT1 in Arabidopsis. Cell 125, 1347-60.

Yin, P., Fan, H., Hao, Q., Yuan, X., Wu, D., Pang, Y., Yan, C., Li, W., Wang, J., and Yan, N. (2009). Structural insights into the mechanism of abscisic acid signaling by PYL proteins. Nat. Struct. Mol. Biol. 16, 1230-6.

Yin, Y., Adachi, Y., Nakamura, Y., Munemasa, S., Mori, I.C., and Murata, Y. (2016). Involvement of OST1 Protein Kinase and PYR/PYL/RCAR Receptors in Methyl Jasmonate-Induced Stomatal Closure in Arabidopsis Guard Cells. Plant Cell Physiol.

## Figure Legends

### Figure 1. Jasmonate signaling precedes stomatal closure upon wounding

(A) Boxplot showing stomatal apertures in response to wounding. Epidermal strips were taken from the abaxial side of leaves that were unwounded or wounded for the indicated time (n indicates number of stomata measured). (B) Boxplot showing the ratiometric quantification of Jas9-VENUS/H2B-RFP fluorescence of epidermal strips shown in (A) indicative for JA signaling efficiency. The boxplots presented show the ratios of the raw integrated densities of Jas9-VENUS fluorescence over the H2B-RFP fluorescence. Adjusted p-values for stomatal opening and Jas9-VENUS/H2B-RFP ratiometric fluorescence analyses are given in tables S1 and S2. The experiment was repeated 3 times with similar results. Boxplots show data for one representative experiment. The confocal images below show a representative image including magnifications for the different time points analyzed.

### Figure 2. GORK mutants are specifically impaired in jasmonate-triggered $K^+$ efflux and stomatal closure

Patch-Clamp experiments showing representative whole cell current densities from guard cell protoplasts of wt Col-0 (left panel) and *gork1-2* mutants (right panel) under control conditions (A) or in response to 1 µM COR (*gork1-2*) or 0.1µM COR (Col-0) (B). Starting from a holding potential of -60 mV voltage pulses in the range from -180 to 100 mV elicited large inward (-90±9 pA/pF at -160 mV) and small outward $K^+$ currents (13±1.7 pA/pF at 100 mV) under control conditions in wt Col-0 guard cells. Under control conditions outward currents were absent in the *gork1-2* mutant. Outward rectifying currents in Col-0 guard cells increased more than 3.5-fold following a 15 min preincubation of guard cell protoplasts with 0.1 µM COR but were absent in *gork1-2* guard cell protoplasts incubated with 1 µM COR. Data represent mean ± S.E, n≥4. (C) I/V plots of Col-0 (left panel) and *gork1-2* (right panel) guard cell $K^+$ current densities. Note the absence of $K^+_{out}$ currents under control (white symbols) as well as COR stimulated (gray symbols) in *gork1-2* guard cells. The inhibition of $K^+_{in}$ currents by COR is reminiscent of ABA action (Yin, et al., 2016) and further supports the notion of JA-ABA crosstalk. Averages from three or more independent experiments are shown. Data represent mean ± S.E, n≥4.
(D, E) Stomatal aperture assays of D) wildtype Col-0, and *gork1-2* or E) wildtype WS and *gork1.* Guard cells were pre-opened in the light for 2 h, then incubated with either 20 µM (±)-ABA or 10 µM MeJA for 1 h. Apertures were determined as the ratio of stomatal width to length. Averages from three or more independent experiments (≥ 80 stomata per bar) are shown. Error bars represent S.E. Asterisks depict significance levels (one asterisk: $p < 0.1$; two asterisks: $p < 0.01$; three asterisks: $p < 0.001$; Mann-Whitney U-test).

### Figure 3. GORK interacts with the CIPK5 kinase and the ABI2 phosphatase

A) Specific interaction of GORK N-terminus with CIPK5 and ABI2 determined by yeast two-hybrid studies as indicated by transactivation of the β-gal reporter activity. Reporter activity is given in Miller units, calculated as the mean value of at least six independent experiments (±S.E.).
B) Bimolecular fluorescence complementation (BiFC) analysis of GORK-$YFP^C$ combined with either $YFP^N$-CIPK5 or $YFP^N$-CIPK15 in transiently transformed *N. benthamiana* epidermal cells. The nucleus region is marked by a white arrow.
C) BiFC analysis of interactions in Arabidopsis mesophyll protoplasts. GORK-$YFP^c$ with CIPK5-$YFP^N$ (left panel), GORK-$YFP^c$ with $YFP^N$-ABI2 (middle panel) and $YFP^C$-ABI2 with CIPK5-$YFP^N$ (right panel).
D) BiFC analysis of $YFP^N$-CIPK5 co-expressed with CBL1-$YFP^C$, CBL9-$YFP^C$ or CBL7-$YFP^C$ in *N. benthamiana* epidermal cells.
E) Localization of GORK-$YFP^C$/$YFP^N$-CIPK5 BiFC complexes upon co-expression with CBL1-OFP in *N. benthamiana* epidermal cells. The distribution of fluorescence was analyzed by scanning fluorescence intensity at the given 'region of interest', which spans the plasma membrane and the nuclei of the depicted cells (white arrows).
Microscopic analyses of transiently transformed *N. benthamiana* epidermal cells were performed 2-3 days after infiltration. Interaction is indicated by yellow fluorescence in B), C) and D), and by green fluorescence in E). In C), the red color represents autofluorescence of chloroplasts. In E), red coloration indicates OFP fluorescence. White bars depict scale bars of 40 µm (B, D, E) or 10 µm (C). Representative images of at least three independent experiments are shown.

**Figure 4. The cytoplasmic N-terminal domain of GORK is phosphorylated by CIPK5 and dephosphorylated by ABI2**

A) CIPK5 phosphorylates the N-terminus but not the C-terminus of GORK. *In vitro* phosphorylation assays were performed in a 1:23 molar ratio of kinase to GORK regions by incubating StrepII-tagged kinase CIPK5 (100 ng) with equivalent molar amounts of the GST-tagged proteins GORK N-terminal domain (amino acids 1 to 67), GORK C-terminus peptide 1 (amino acids 301 to 559) or GORK C-terminus peptide 2 (amino acids 531 to 820).
B) ABI2 directly dephosphorylates the N-terminal domain of GORK. *In vitro* phosphorylation assays were performed with StrepII-tagged CIPK5 (75 ng), an equivalent molar amount of StrepII-tagged ABI2 and GST-tagged GORK N-terminus (1500 ng). CIPK5 - GORKNT *in vitro* kinase reactions shown in lanes 6 and 7 were performed for 30 min before StrepII-ABI2 protein (lane 6) or buffer control (lane 7) were added and reactions were incubated for an additional 30 min.

**Figure 5. Antagonistic regulation of GORK by ABI2 and CBL1/9-CIPK5**

A) Electrophysiological characterization of GORK activity upon co-expression with the phosphatase (ABI2), kinase (CIPK5) and $Ca^{2+}$-sensors (CBL1). Whole-oocyte currents recorded upon 3 s voltage pulses ranging from -100 to +60 mV in 20 mV increments, using a holding potential of -40 mV. Expression of GORK (left trace) resulted in the typical slow activation of the *Shaker*-type channel. Co-expression with ABI2 reduced GORK currents (middle). Addition of CIPK5 and CBL1 counteracted ABI2-inhibition (right). Current traces of representative cells are shown.

B) Current-voltage plot of steady-state currents ($I_{SS}$) of GORK (▪), GORK co-expressed with ABI2 (●) or GORK co-expressed with ABI2, CIPK5 and CBL1 (△). Data represent mean currents ± S.E. from n ≥ 6 experiments.

C) Phosphatase specificity. Normalized steady-state currents at 60 mV from oocytes expressing GORK or GORK with either ABI1 or ABI2. ABI2 significantly inhibited GORK activity by 74±1.9 %. ABI1 had no significant effect on GORK (11.9±8.6 %). Results represent mean values ± S.E. of 14 or more oocytes.

D) Kinase specificity. Co-expression of either CIPK5 or CIPK15 with CBLs revealed that only CIPK5 is able to partly reverse GORK inhibition by ABI2. CIPK5 activity depended on the presence of either CBL1 or CBL9, whereas CIPK15 in combination with a mix of CBL1, CBL4, CBL5 and CBL9 failed to antagonize ABI2 inhibition of GORK (n ≥ 7 oocytes, mean values ± S.E).

E) $Ca^{2+}$- and phosphorylation-dependent channel activation by CBL1/9-CIPK5 complex. Co-expression CIPK5 mutants impaired in kinase activity (CIPK5 K41N or CIPK5 D153N) failed to release ABI2-dependent inhibition of GORK activity. Likewise, CBL1 mutants affected in either plasma membrane targeting (CBL1 G2A) or $Ca^{2+}$ binding (CBL1 EF1-4 or CBL1 E172Q) were also impaired in GORK activation. Note that a point mutation in EF hand four (CBL1 E172Q) was less significant compared to the CBL1 EF1-4 mutant affected in all four EF-hands. (n ≥ 8 oocytes, mean values ± S.E). Asterisks depict significance levels (two asterisks: $p < 0.01$; three asterisks: $p < 0.001$; Mann-Whitney U-test).

.

**Figure 6: CIPK5 is essential for JA-mediated GORK activation and stomatal closure**

Patch-Clamp experiments showing representative whole cell current densities from guard cell protoplasts of *cipk5-2* mutants under control conditions (A) or in response to 0.1 µM COR (B). Experimental procedures were as in Fig. 2. (C) I/V plots of guard cell $K^+$ current densities under control conditions (open symbols) and after COR treatment (closed symbols); (n(ctrl)=16, n(COR)=6; mean ± SE). Inhibition of $K^+_{in}$ current density by COR at -140 mV is 59±12%, $p<0.005$. (D) Guard cell responses of *cipk5-2, cbl1/9, abi1-1 and abi2-1* mutants towards ABA or MeJA. Stomata were pre-opened under light for 2 h, then incubated with 20 µM (±)-ABA or 10 µM MeJA for 1 h. Averages from three or more independent experiments (≥ 80 stomata per bar) are shown. Error bars represent S.E. (E) Stomatal aperture assays of Col-0, and *gork1-2* in response to wounding. Guard cells were pre-opened in the light for 2 h, then wounded using forceps. Apertures were determined after 1h in local and systemic (position +3 relative to local) leaves as the ratio of stomatal width to length. Averages from three or more independent experiments (≥ 80 stomata per bar) are shown. Error bars represent S.E.

**Figure 7. Working model of the convergence of JA and ABA-mediated stomatal closure**
Upon binding to their respective receptors COI1 and the PYR/PYLs, both JA and ABA increase cytosolic $Ca^{2+}$ levels. Activated ABA receptors recruit the PP2Cs ABI1 and ABI2 to the receptor complex, thereby inactivating phosphatase activity. This enables phosphorylation and release of kinases such as OST1 ($Ca^{2+}$-independent), or CIPKs and CPKs ($Ca^{2+}$-dependent). Importantly, ABI2 no longer inhibits the GORK channel. OST1 dependent inhibition of KAT1 and kinase activation of anion channels (SLAC1/SLAH/QUAC) leads to membrane potential depolarization, and in turn, activation of the voltage dependent GORK channel. CBL1/9-CIPK5 dependent GORK activation further promotes potassium efflux and thus stomatal closure. A role for JA co-receptors of the JAZ family in this process is currently unreported. JA however affects ABA biosynthesis and/or signaling leading $Ca^{2+}$-dependent activation of the and in turn GORK phosphorylation. For the sake of clarity, we have not included ABA/JA-stimulated ROS production via respiratory burst oxidase homologs (RBOHs). It should be noted however that $H_2O_2$ further stimulates GORK activity while at the same time inhibiting ABI2 activity (Meinhard et al., 2002).

## STAR Methods

### CONTACT FOR REAGENT AND RESOURCE SHARING

Further information and requests for resources and reagents should be directed to and will be fulfilled by the Lead Contact, Dirk Becker (dirk.becker@uni-wuerzburg.de).

### EXPERIMENTAL MODEL AND SUBJECT DETAILS

#### Plant material

*Arabidopsis thaliana* plants were cultivated on common potting soil in climate growth chambers under long-day conditions (12-hour light 24°C/12-hour dark 18°C) at a light intensity of 120 µmol s−1 m−2 and 50% relative humidity. Genotype of mutant lines was verified with genotyping primers as indicated by SIGnaL T-DNA primer design

(http://signal.salk.edu/tdnaprimers.2.html, Salk Institute Genomic Analysis Laboratory, LaJolla, CA, USA).

For wounding experiments, Jas9-VENUS expressing plants Arabidopsis plants were grown for 4 weeks in short days (8-hour light 21°C/16-hour dark 19°C) at a light intensity of 120 µmol s−1 m−2 and 50% relative humidity. Epidermal strips were taken from leaf #6 (wounded leaf) or leaf #9 (systemic leaf) (ref: https://www.nature.com/protocolexchange/protocols/2787) at different time points after wounding and imaged directly after.

For stomatal aperture assays, excised rosette leaves of 5- to 6-week-old plants were used, while for guard cell isolation epidermal peels of rosette leaves from about 4-week-old plants were used (more information in the METHOD DETAILS section).

For fluorescence microscopy, mesophyll cells of 4- to 5-week-old *A. thaliana* rosette leaves of were isolated by enzymatic digestion (details on protoplastation in the METHOD DETAILS section).

*Nicotiana benthamiana* plants were cultivated in a glasshouse under long day conditions (12-hour light /12-h dark) with 60% atmospheric humidity. Leaves of 5-6 weeks old plants

For abscisic acid concentration assays, 19-20 days old ABAleon2.1 expressing seedlings were grown on 0.5 MS-agar (1% agar, 0.5X Murashige and Skoog Basal Salt Mixture, 1% sucrose) in a plant growth chamber (Conviron Europe Ltd, Isleham, United Kingdom) at 22 °C and 100 µM/$m^2$s.

**Xenopus oocyte preparation**

Investigations on GORK channel regulation were performed in oocytes of the African clawfrog *Xenopus laevis*. Permission for keeping *Xenopus* exists at the Julius-von-Sachs Institute and is registered at the government of Lower Franconia (reference number 70/14). Mature female *X. laevis* frogs were kept at 20°C at a 12/12 h day/night cycle in dark grey 96-liter tanks (5 frogs/tank). Frogs were fed twice a week with floating trout food (Fisch-Fit Mast 45/7 2mm, Interquell GmbH, Wehringen, Germany). Tanks were equipped with 30 cm long PVC pipes with a diameter of around 10 cm that serve as hiding places for the frogs and a small standard aquarium pump for continuous water circulation and filtration. Water was changed and tanks as well as pumps were cleaned weekly. For partial ovariectomy, mature frogs were anesthetized by immersion in water containing 0.1% 3-aminobenzoic acid ethyl ester. Stage V or VI oocytes were treated with 0.14 mg/ml collagenase I in $Ca^{2+}$-free ND96 buffer (10 mM HEPES pH 7.4, 96 mM NaCl, 2 mM KCl, 1 mM $MgCl_2$,) for 1.5 h. Oocytes were washed with $Ca^{2+}$-free ND96 buffer and kept at 16°C in ND96 solution (10 mM HEPES pH 7.4, 96 mM NaCl, 2 mM KCl, 1 mM $MgCl_2$, 1mM $CaCl_2$) containing 50 mg/l gentamycin. For electrophysiological experiments, 15 ng of each cRNA was injected into selected oocytes with a nanoinjector (Drummond Scientific Company, Broomall, PA, USA). Oocytes were incubated for 3 to 5 days at 16°C in ND96 solution containing gentamycin before measurements.

**METHOD DETAILS**

**Jas9-VENUS imaging and fluorescence quantification**

Epidermal strips were taken from the abaxial side of leaves that were unwounded (mock controls) or crush-wounded for the indicated time using forceps. Epidermal strips were

dissected and immediately imaged on an upright Leica SP5 confocal laser scanning microscope (Leica Microsystems, Wetzlar, Germany). Scanner and detector settings used for one experiment were optimized to avoid saturation and to maximize resolution and kept unchanged throughout the experiment. VENUS was excited using the 514 nm line of an argon laser and the fluorescence collected from 520 to 560 nm. RFP was excited using a 561-nm laser diode and the fluorescence collected from 590 to 680 nm. Brightfield images were also collected to measure stomatal opening. Fluorescence quantification was performed as described in Larrieu et al. (2014). Briefly, background fluorescence was removed using a threshold and only fluorescence coming from the nuclei was quantified using Fiji software (ImageJ 1.51a).

**Patch-Clamp Experiments**

Guard Cell Protoplastation

Epidermal peels of rosette leaves from about four weeks old Arabidopsis plants were incubated for 16 h at 18 °C in enzyme solution composed of 0.65% (wt/vol) cellulase Onozuka-R10 (Serva), 0.35% (wt/vol) macerozyme Onozuka-R10 (Serva), 0.4 M sorbitol, 0.05 mM KCl, 0.05 mM CaCl2, 5 mM ascorbic acid, 0.05% (wt/vol) kanamycin sulfate (Fluka) and adjusted to pH 5.5 MES/Tris. Then, the suspension was filtered through a 50 µm nylon mesh, washed with washing solution (20 mM CaCl2, 5 mM MES-Tris, pH=5.6, adjusted to an osmolality of 400 mosmol/kg with D-sorbitol) and centrifuged at 600 xg and 4 ◦C for 10 min. The supernatant was discarded immediately and the enriched protoplasts were stored on ice in measuring

chambers as samples of 50 µl (plus 250 µl washing solution) for minimum 1 h before they were used for patch-clamp experiments.

Patch Clamp Recordings

The whole-cell patch clamp configuration was established on guard cells isolated from epidermal peels as previously described by Geiger et al. (2010). Macroscopic current recordings were performed at a sampling rate of 100 µs and low-pass filtered at 1.3 kHz using an EPC7 patch clamp amplifier (HEKA Electronic, Lambrecht, Germany). From a holding potential of −60 mV, voltage pulses ranging from −180 to +100 mV were applied in 20-mV steps for 1 s. The standard bathing solution contained 10 mM KCl, 10 mM $CaCl_2$, 2 mM $MgCl_2$ and 0.5 mM $LaCl_3$ adjusted to pH 5.6 with 5 mM MES/TRIS and to an osmolality of 400mOsmol·$kg^{-1}$ with D-sorbitol. The standard pipette solution facing the cytosolic side of the plasma membrane comprised 100 mM KGlu, 4.5 mM $CaCl_2$, 5 mM EGTA (corresponding to 1 µM free calcium) and 2 mM $Mg_2ATP$, adjusted to pH 7.4 with 10 mM HEPES/TRIS, with an osmolality of 440 mOsmol·$kg^{-1}$ using D-sorbitol. To study the effect of JA on $K^+$ channel activity guard cell protoplasts were preincubated with 0.1-1µM coronatine in washing solution (20 mM $CaCl_2$, adjusted to pH=5.6 using 5 mM MES/Tris with an osmolality of 400 mOsmol·$kg^{-1}$ using D-sorbitol) for 15min on ice. Note that in contrast to stomatal aperture assays we here used COR rather than MeJA. We noticed that under Patch-Clamp conditions where protoplasts are continuously superfused with bath solution MeJA, due to its volatile and lipophilic character, stuck to the superfusion system and we thus had no control about the actual MeJA concentration in the recording chamber. Steady state current amplitudes

were determined at the end of each voltage pulse and normalized to the membrane capacitance of individual guard cell protoplasts.

**Stomatal aperture measurements**

*Arabidopsis thaliana* ecotypes Columbia-0 (Col-0), Landsberg *erecta* (L*er*) and Wassilewskija (Ws) were employed as wildtype plants, corresponding to the tested mutant backgrounds (see KEY RESOURCES TABLE for additional information on mutant lines). Intact rosette leaves were incubated for 2 h in the light in a medium containing 10 mM MES-KOH, pH 6.15, 10 mM KCl and 50 µM $CaCl_2$ to promote stomatal opening. ABA, MeJA, the peptide flg22 (Felix, et al., 1999) or 0.1 % methanol (control) were added directly to the buffer. After 1 h, stomatal aperture was determined using a digital microscope (Keyence vhx, Keyence Corporation, Osaka, Japan) at 2,000x magnification. The length and width of ≥ 20 stomata per leaf were measured using Image J software (Image J 1.47, Wayne Rasband, National Institute of Health, USA), which allowed the calculation of the aperture ratio (width/length). At least two independent experiments were performed per plant and condition.

**Yeast two-hybrid studies**

Interaction studies yeast transformation and two-hybrid analyses were performed using yeast strain HF7c (Himmelbach et al.; 2002). In brief: the cDNA sequence of GORK-NT (amino acid 1-36) was cloned into the pGAD424 yeast expression vector (Takara Bio Europe S.A.S., Goteborg, Sweden; GenBank Accession #: U07647). Full-length cDNA sequences of CIPKs (CIPK4, 5, 6, 7, 8, 13, 15 and 23) and ABI1 and ABI2 were amplified by PCR and cloned into

pGBT9 (Takara Bio Europe S.A.S., Goteborg, Sweden, GenBank Accession #: U07646). In interaction studies GORK-NT was used as bait, with CIPKs and PP2Cs as prey. For CBL-CIPK5 studies the coding sequences of CIPKs and CBLs were introduced into the activation domain (AD) plasmid (pGAD.GH) and the DNA-binding domain (BD) plasmid (pGBT9.BS), respectively (Kolukisaoglu et al., 2004; Albrecht et al., 2001). CIPK-CBL yeast two-hybrid studies were conducted as described previously (Hashimoto et al., 2012).

**Bimolecular fluorescence complementation (BiFC) studies.**

BiFC experiments were either performed in *N. benthamiana* epidermis cells or *A. thaliana* mesophyll protoplasts.

Preparation of constructs

The coding sequences of *CIPK5* and *CIPK15* were fused to the N-terminal (in the vector pSPYNE(R)173), and the coding sequence of *GORK* to the C-terminal (in the vector pSPYCE(M)) fragment of eYFP (Waadt, et al., 2008), leading to the constructs $YFP_N$-CIPK5, $YFP_N$-CIPK15, GORK-$YFP_C$. The coding sequences of CBL1, CBL9 and CBL7 were fused to the C-terminal fragment of eYFP in the vector pSPYCE(M) leading to CBL1-$YFP_C$, CBL7-$YFP_C$, and CBL9-$YFP_C$, as described previously (Hashimoto et al., 2012). The CBL1-OFP construct was generated from pMAS-CBL1.HA (Batistic et al., 2008) by replacing the HA-tag with OFP. The PM marker CBL1n-OFP was generated by fusion of the first 12 amino-acids of CBL1 to OFP Held (Held, et al., 2011). ABI2 was fused with either $YFP_C$ or $YFP_N$, resulting in $YFP_C$-ABI2 and $YFP_N$-ABI2. These

constructs were cloned via the USER-technique (see details in “Cloning and cRNA synthesis”) into a modified pCAMBIA binary vector containing a pUBQ10 promoter.

*A. thaliana* protoplastation and transient transformation

Mesophyll protoplasts were isolated from 4-6-week-old *Arabidopsis thaliana* Col-0. Rosetta leaves were incubated for 3 h in dark in enzyme solution (1-1.5 % cellulase R10, 0.1-0.4% macerozyme R10, 0.4 M mannitol, 20 mM KCl, 20 mM MES, pH 5.7, 10 mM $CaCl_2$, 0.1% BSA). The enzyme solution containing protoplasts was filtered with a 50 µm nylon mesh with W5 buffer (154 mM NaCl, 125 mM $CaCl_2$, 5 mM KCl, 2 mM MES pH 5.7). After pelleting the protoplasts at 100 x g for 2 min, the isolated protoplasts were incubated on ice for 30 min in 2 ml W5 buffer. Buffer was replaced by MMg solution (4 mM MES pH 5.7, 0.4 M mannitol, 15 mM $MgCl_2$) and incubated for 15 min at RT. For transient transformation, 15 µg plasmid DNA per BiFC construct, 200 µl protoplast solution and 220 µl PEG solution (PEG 4000, 0.2M Mannitol, 0.1 M $CaCl_2$) were mixed gently and incubated for 15 min at RT. After adding 800 µl W5 the reaction was centrifuged at 100 g for 1 min. The supernatant was removed, and the protoplasts were kept in 2 ml W5 buffer in the dark and at RT for 2 days.

Transient transformation of *N. benthamiana* epidermis cells

Leaves of *N. benthamiana* were infiltrated with *Agrobacterium tumefaciens* (GV3101 with helper plasmid pMP90) that were previously transformed with respective plant expression vectors. The *Agrobacterium* strains were infiltrated at an OD600 of 0.5 for the ones transformed with BiFC constructs and at an OD600 of 0.3 for those transformed with the helper plasmid or the CBL1-OFP and CBL1n-OFP constructs. After incubation under continuous

light for 48 hours, leaf discs of infiltrated leaves were excised using a cork-borer and used for microscopic analysis.

Fluorescence microscopy

Analysis of protein interactions and subcellular localization studies were performed by confocal laser scanning microscopy (Leica inverted microscope DMIRE2, equipped with a Leica TCS SP2 laser scanning device, or Leica inverted microscope DMI6000 with a Leica TCS SP5 II laser scanning device (Leica Microsystems GmbH, Wetzlar, Germany)). For excitation of YFP constructs, an argon laser was used, whereas fluorescence emission was detected between 520 and 550 nm. mOrange fusion proteins were excited with a 562 nm diode laser and mOrange fluorescence emission was detected between 560 and 620 nm. Chlorophyll autofluorescence was detected at 630 to 750 nm. Images were processed and color optimized using Leica Application Suite X, Fiji (ImageJ 1.51a) and Adobe Photoshop.

### *In vitro* phosphorylation assays

Cloning procedures and phosphorylation assays

For expression of N-terminally GST-tagged proteins, the sequence of the GORK N-terminus (amino acids 1 to 67) was amplified and introduced into the vector pET-GST (Drerup et al., 2013), and the sequences of GORK C-terminus peptide 1 (P1, amino acids 301 to 559) and peptide 2 (P2, amino acids 531 to 820) were cloned into pGEX-6P-1 (GE Healthcare, Chicago, IL, USA). Recombinant proteins of GST-GORKNT and of GST-GORKCT P1/P2 were overexpressed in *Escherichia coli* BL21 CodonPlus(DE3)-RIL (Stratagene California, La Jolla, CA, USA) and Rosetta (DE3)pLysS (Merck KgaA, Darmstadt, Germany) cells, respectively, and

affinity- purified using Glutathione HiCap Matrix (QIAGEN, Hilden, Germany). GST-GORKNT was purified from the supernatant after centrifugation of the lysed cell extract. Purification of GST-GORKCT peptides was performed from the post-sonicate pellet after solubilization with 6 M urea and in the presence of 1 mM Brij 35, as previously described (Drerup et al., 2013).

For expression of the StrepII-CBL1 and StrepII-ABI2, the coding sequences of CBL1 and ABI2 were amplified, fused to an N-terminal StrepII-tag and cloned into pET24b(+) vector. StrepII-CBL1 and StrepII-ABI2 were overexpressed in *E. coli* BL21 CodonPlus(DE3)-RIL cells, and purified from the supernatants after cell lysis and centrifugation using Strep-Tactin MacroPrep (IBA Lifesciences GmbH, Göttingen, Germany). To obtain StepII-tagged CIPK5 protein, the coding sequence of CIPK5 was cloned into the pIVEX-WG-STREPII vector (Hashimoto et al., 2012). The protein was expressed using the RTS 500 wheat germ CECF kit (biotechrabbit GmbH, Hennigsdorf, Germany) following the manufacturer's instructions, with the exception that 0.5 mM Brij 35 was added during the *in vitro* transcription/translation reaction. Subsequently, StrepII-CIPK5 protein was purified using Strep-Tactin MacroPrep (IBA Lifesciences GmbH, Göttingen, Germany).

Phosphorylation assays

For *in vitro* phosphorylation assays, purified proteins in their respective elution buffer were incubated in 24 µl reactions for 30 min at 30 °C. The reaction buffer contained 5 mM $MnSO_4$, 0.5 mM $CaCl_2$, 2 mM DTT, 10 µM ATP and 4 µCi of [$\gamma$-$^{32}$P] ATP (3000 Ci/mmol). For studying the influence of ABI2 on GORK N-terminus phosphorylation, StrepII-ABI2 protein or buffer control were subsequently added for an additional 30 min. Reactions were stopped with 5x concentrated Laemmli sample buffer and loaded on gels for SDS-polyacrylamide gel

electrophoresis. Gels were fixed by Coomassie staining and radioactively labeled proteins were visualized by autoradiography.

**Cloning and cRNA synthesis**

For heterologous expression in *Xenopus* oocytes, the cDNAs of GORK, ABI1, ABI2, CIPK5, CIPK15, CBL1 and CBL9 were cloned with gene-specific oligonucleotide primers into oocyte expression vectors (based on pNBIu vectors, see KEY RESOURCES TABLE) by an advanced uracil excision-based cloning technique described by Nour-Eldin et al. (2006). Site-directed mutagenesis was performed to generate CIPK5$^{K41N}$, CIPK5$^{D153N}$, CBL1$^{E172Q}$ and CBL1$^{E56Q\ D91N\ E128Q\ E172Q}$ (CBL1 EF1-4) with the same uracil-excision-based cloning technique. Amplification of the coding sequences was performed using Phusion F530 polymerase (Thermo Fisher Scientific Inc., Waltham, MA, USA), and the USER reaction of PCR product and its target plasmid was performed with USER enzyme (New England Biolabs, Ipswich, MA, USA), both according to the manufacturers' protocols. The resulting constructs were immediately transformed into chemically competent *Escherichia coli* cells (XL1-Blue MRF'), and subsequently verified by sequencing. For functional analysis, cRNAs were prepared with the AmpliCap-Max T7 High Yield Message Maker Kit (Cellscript, Madison, WI, USA) by following the manufacturer's instructions. Oocyte preparation and cRNA injection have been described in EXPERIMENTAL MODEL AND SUBJECT DETAILS.

**Xenopus oocyte recordings**

GORK channel activity was recorded in TEVC measurements on oocytes exposed to a bath solution (10 mM KCl, 90 mM LiCl, 1 mM $CaCl_2$, 1 mM $MgCl_2$, 10 mM Hepes-NaOH pH 7.5) with the software WinWCP V4.4.7 (Strathclyde Electrophysiology Software, University of Strathclyde, Glasgow, United Kingdom). Starting from a holding potential of -40 mV, cells were pre-clamped to -80 mV for 1 s, and 3 s single-voltage pulses were subsequently applied in 10 mV increments from −100 mV to +60 mV. To allow normalization and comparison of the various channel/phosphatase/kinase combinations tested in this paper, GORK, GORK with ABI2, and GORK, ABI2, CIPK5/CBL1 were always measured to calibrate the current responses of the CIPK5 and CBL1 mutants. Recorded current data were normalized to the 60 mV response of GORK. At least three technical replicates were performed per combination.

**Total RNA extraction and quantitative PCR (qPCR).**

RNA was isolated from eight biological replicates for each condition, with two replicates pooled prior to RNA extraction, resulting in four samples per condition total. Rosetta leaves of 4-5-week-old Arabidopsis plants were cut off for guard cell enrichment. Subsequently, mid veins were excised and discarded. Leaf material was minced in a standard blender (4142 MX32, Braun GmbH, Kronberg, Germany) with 300 ml ice-cold $H_2O$ for 45 s. Epidermis fragments were collected in a 120 µm filter mesh. Blending was repeated, and the residual plant tissue was carefully dried with a paper towel before the pellet was transferred into a 2 ml Eppendorf reaction tube and then frozen in liquid nitrogen. RNA was extracted using the E.Z.N.A. Plant RNA Kit (Omega Bio-Tek, Inc., Norcross, GA, USA), according to the

manufacturer's protocol, with the exception that RNA was eluted twice with 12 µl RNAse-free $H_2O$. Quality control measurements were performed on an Experion$^{TM}$ automated electrophoresis station (Bio-Rad Hercules, CA, U.S.A.) and the concentration was determined using a Nanodrop ND-1000 spectrophotometer (Thermo Fisher Scientific, Wilmington, DE, U.S.A.). A total of 2.5 mg of RNA was DNase-digested using RNase-free DNase I (Fermentas/Thermo Fisher Scientific Inc., Waltham, MA, USA). Following precipitation with 5 M $NH_4Cl$ in isopropanol and washing with 70% ethanol, RNA was reverse transcribed using MMLV virus RNase H2 Reverse Transcriptase (MLV-RT; Promega Corporation, Madison, Wisconsin, USA) according to the manufacturer's protocol. At least three guard cell samples were measured in three technical replicates in a Mx3005P thermal cycler (Stratagene, La Jolla, CA, USA). Gene-specific primer pairs (TIB MOLBIOL Syntheselabor GmbH, Berlin, Germany) were designed to amplify small fragments not exceeding 500 bp and validated prior to qPCR. Transcript amounts were standardized in relation to UBC21 transcripts and displayed relative to the expression level in the control treatment. Primers are listed in Table S3.

**Recording of abscisic acid concentration changes.**

ABA measurements in guard cells using the FRET-based ABA reporter ABAleon2.1 were performed as described elsewhere (Waadt et al., 2014). Four leaves of 19- to 20-day-old-plants were detached and floated on incubation buffer (5 mM KCl, 50 µM $CaCl_2$, 10 mM MES-Tris pH 5.6) at 22 °C and 100 µmol $m^{-2}$ $s^{-1}$ for 2 h. Leaves were treated with either 10 µM (+)-ABA, 10 µM MeJA or 0.01 % ethanol for 1h and leaf epidermal tissue was collected using the

blending method. Excised leaves were blended with a standard commercial blender for 15s, then passed through a filter mesh and blended a second time for 15s. Epidermal fragments were mounted on a microscope slide for imaging. Fluorescence emission of mTurquoise (465-505 nm) and cpVenus173 (520-550 nm) was recorded using a laser scanning microscope after excitation at 458 nm (Leica TCS SP5II; Leica Microsystems GmbH, Wetzlar, Germany). Experiments were performed twice in triplicates with blind treatments. Images were processed (emission ratio calculation), analyzed and calibrated using Fiji software (Schindelin et al., 2012).

**QUANTIFICATION AND STATISTICAL ANALYSIS**

All results were gained from ≥ two independent experiments. Results are given as mean ± standard deviation (SD) or standard error (SE). Detailed information on what n represents, the statistical tests used in the particular analysis and other information are indicated in the figure legend. Statistical significance was tested with either a student's t-test or Mann-Whitney U-test. The pairwise comparison in the Jas9- stomatal aperture experiment was done using Dunn's-test for multiple comparisons of independent samples and the P values were adjusted using holm's method.

Significance levels are depicted in the figures with asterisks and were coded as followed: one asterisk – $p < 0.05$, two asterisks – $p < 0.01$, three asterisks – $p < 0.001$. For statistical analysis and graph preparations Igor Pro 6 (WaveMetrics, Inc., Lake Oswego, Oregon, USA), Origin Pro 2016 (OriginLab Corporation, Northampton, MA, USA) the programming language R Version 3.1.0 or 3.1.2 (R Development Core Team, Vienna, Austria), Excel (Microsoft Corp. Redmond,

WA, USA) and CorelDRAW (Corel Corporation, Ottawa, Ontario, Canada) were used. Fluorescence images were analyzed, processed and calibrated with Leica Application Suite X (Leica Microsystems GmbH, Wetzlar, Germany), Fiji (ImageJ 1.47 or 1.51a; Wayne Rasband, National Institute of Health, USA) and Adobe Photoshop (Adobe Systems Inc., San José, CA, USA).

**DATA AND SOFTWARE AVAILABILITY**

Software used in this study is listed in the KEY RESOURCES TABLE and QUANTIFICATION AND STATISTICAL ANALYSIS section.

**Supplemental Videofiles**

VideoS1, related to Fig. 1A shows wound induced stomatal closure after a neighboring stoma of the monitored stoma was wounded using a sharp micro-electrode. The movement was recorded until 30 min after wounding.

## KEY RESOURCE TABLE

| REAGENT or | SOURCE | IDENTIFIER |
|---|---|---|
| Bacterial and Virus Strains | | |
| XL1-Blue MRF' *E. coli* strain used for cloning | Widely distributed | N/A |
| BL21 CodonPlus(DE3)-RIL *E. coli* strain for overexpression | Stratagene | N/A |
| Rosetta (DE3)pLysS *E. coli* strain for overexpression | Merck KGaA | Cat# 70956-3 |
| Biological Samples | | |
| *A. thaliana* Col-0 | Lehle Seeds USA | WT-02-45-02 |
| *A. thaliana* Wassilewskija (Ws-0) | Lehle Seeds USA | WT-08A |
| *A. thaliana* Landsberg *erecta* (Ler-0) | Lehle Seeds USA | WT-04 |
| *Nicotiana benthamiana* | Widely distributed | N/A |
| *Saccharomyces cerevisiae* | Widely distributed | HF7c |
| Chemicals, Peptides, and Recombinant Proteins | | |
| Gentamicin sulfate salt | Sigma-Aldrich, Merck | Cat# G1264 |
| Kanamycin sulfate salt | Fluka, Sigma-Aldrich | N/A |
| Standard chemicals such as salts and buffers for electrophysiological recordings or for molecular biology | Sigma-Aldrich, Merck | N/A |
| USER-Enzyme | New England Biolabs | Cat# M5505 |
| Phusion F530 polymerase | Thermo Fisher Scientific | Cat# F530S |
| Brij 35 | Merck Millipore | CAS 9002-92-0, Cat# 8019620250 |
| Poly(ethylene glycol) average Mn 4,000, platelets (PEG) | Sigma-Aldrich, Merck | Cat# 81240 |
| CELLULASE "ONOZUKA" R-10 | Serva Electrophoresis GmbH, Heidelberg | Cat# 16419 |
| MACEROZYME R-10 | Serva *E*lectrophoresis GmbH, Heidelberg | Cat# 28302 |
| Critical Commercial Assays | | |
| Glutathione HiCap Matrix | QIAGEN | Cat# 30900 |
| E.Z.N.A. Plant RNA Kit | Omega Bio-Tek | Cat# R6827-00 |
| AmpliCap-Max T7 High Yield Message Maker Kit | Cellscript, Madison, WI, USA | Cat# C-MSC100625 |
| Strep-Tactin MacroPrep | IBA Lifesciences | Cat# 2-1505-010 |
| RTS 500 Wheat Germ CECF Kit | biotechrabbit | Cat# BR1401101 |
| Experimental Models: Organisms/Strains | | |
| *A. thaliana* Col-0 | Lehle Seeds USA | WT-02-45-02 |

| REAGENT or | SOURCE | IDENTIFIER |
|---|---|---|
| *A. thaliana* Wassilewskija (Ws-0) | Lehle Seeds USA | WT-08A |
| *A. thaliana* Landsberg *erecta* (Ler-0) | Lehle Seeds USA | WT-04 |
| *A. thaliana* (Ws) *gork1* | Herve Sentenac, ENSAM, Montpellier, France | FLAG_064H07 |
| *A. thaliana* (Col-0) Jas9-VENUS | Larrieu et al., 2015 | N/A |
| *A. thaliana* (Col-0) *gork1-2* | NASC | GABI_865F05 |
| *A. thaliana* (Ler) *abi1-1*; ABA-insensitive point mutation | Koornneef et al., 1984 | N/A |
| *A. thaliana (Ler) abi2-1;* ABA-insensitive point mutation | Rodriguez et al., 1998 | N/A |
| *A. thaliana* (Ws) *cbl1* | NASC | NASC ID: N1601 |
| *A. thaliana* (Col-0) *cbl9* | Pandey et al. 2004 | N/A |
| *A. thaliana* (Ws x Col-0) *cbl1/cbl9* | Cheong et al., 2007 | N/A |
| *A. thaliana* (Col-0) *abi2-2* | Rubio et al., 2007 | SALK_015166 |
| *A. thaliana* (Col-0) *abi1-2/abi2-2* | Rubio et al., 2009 | N/A |
| *A. thaliana* (Col-0) *coi1-16* | NASC | NASC ID: N67817 |
| *A. thaliana* (Col-0) *aba3-1*; point mutation | NASC | NASC ID: N157 |
| *A. thaliana* (Col-0) *pyr/pyl1245* | Gonzalez-Guzman et al. 2012 | N/A |
| *A. thaliana (Ler) ost1-2* | Mustilli et al., 2002 | N/A |
| *A. thaliana* (Col-0) *slac1-3* | NASC | SALK_099139 |
| *A. thaliana* (Col-0) *cipk5-1* and complementation lines | NASC; this paper | SALK_063555 |
| *A. thaliana* (Col-0) *cipk5-2* and complementation lines | NASC; this paper | SALK_084455 |
| *A. thaliana (*Col-0) ABAleon2.1 | Waadt et al., 2014 | N/A |
| *Nicotiana benthamiana* | Widely distributed | N/A |
| Oligonucleotides | | |
| CDS cloning primers | synthesized by Sigma-Aldrich, Merck, Germany | N/A |
| See Table S3 for qPCR primers | synthesized by TIB Molbiol Berlin, Germany | This paper |
| Genotyping primers | synthesized by Sigma-Aldrich, Merck, Germany | http://signal.salk.edu/tdnaprimers.2.html |
| Recombinant DNA | | |
| Oocyte expression vector | Nour-Eldin et al., 2006 | pNB1u |
| Yeast 2 Hybrid expression vector | Clontech | pGAD424 |
| Yeast 2 Hybrid expression vector | Takara/Clontech | pGBT9 |
| Yeast 2 Hybrid expression vector | Takara/Clontech | pGBT9.BS |

| REAGENT or | SOURCE | IDENTIFIER |
|---|---|---|
| Yeast 2 Hybrid expression vector | Takara/Clontech | pGAD.GH |
| Bacterial overexpression vector | Addgene | pET-GST |
| Bacterial overexpression vector | GE Healthcare | pGEX-6P-1 |
| Binary plant expression vector | | pGPTVII |
| Plant expression vectors pSPYCE (M) and pSPYNE (R) 173 for co-localization studies | Waadt et al., 2008 | pSPYCE (M) and pSPYNE (R) 173 |
| Plant expression vector for co-localization studies; modified to allow USER cloning | Cambia | pCambia |
| Bacterial overexpression vector | Merck Millipore | pET-24b(+) |
| CDS of GORK and its interactors were cloned into pNB1u, pET-GST, pGEX-6P-1, pet24b(+), pGAD424, pGPTVII or pCambia for electrophysiological analysis, Y2H, phosphorylation or localization studies | This study; Hashimoto et al., 2012; Maierhofer et al., 2014 | N/A |
| Vector for cell free *in vitro* transcription/translation in wheat germ lysate | Hashimoto et al., 2012 | pIVEX-WG-StrepII |
| Software and Algorithms | | |
| PATCHMASTER | https://www.heka.com | N/A |
| Fiji – ImageJ | https://fiji.sc | N/A |
| IGOR Pro | https://www.wavemetrics.com | N/A |
| WinWCP V4.4.7 (Strathclyde Electrophysiology Software) | University of Strathclyde | N/A |

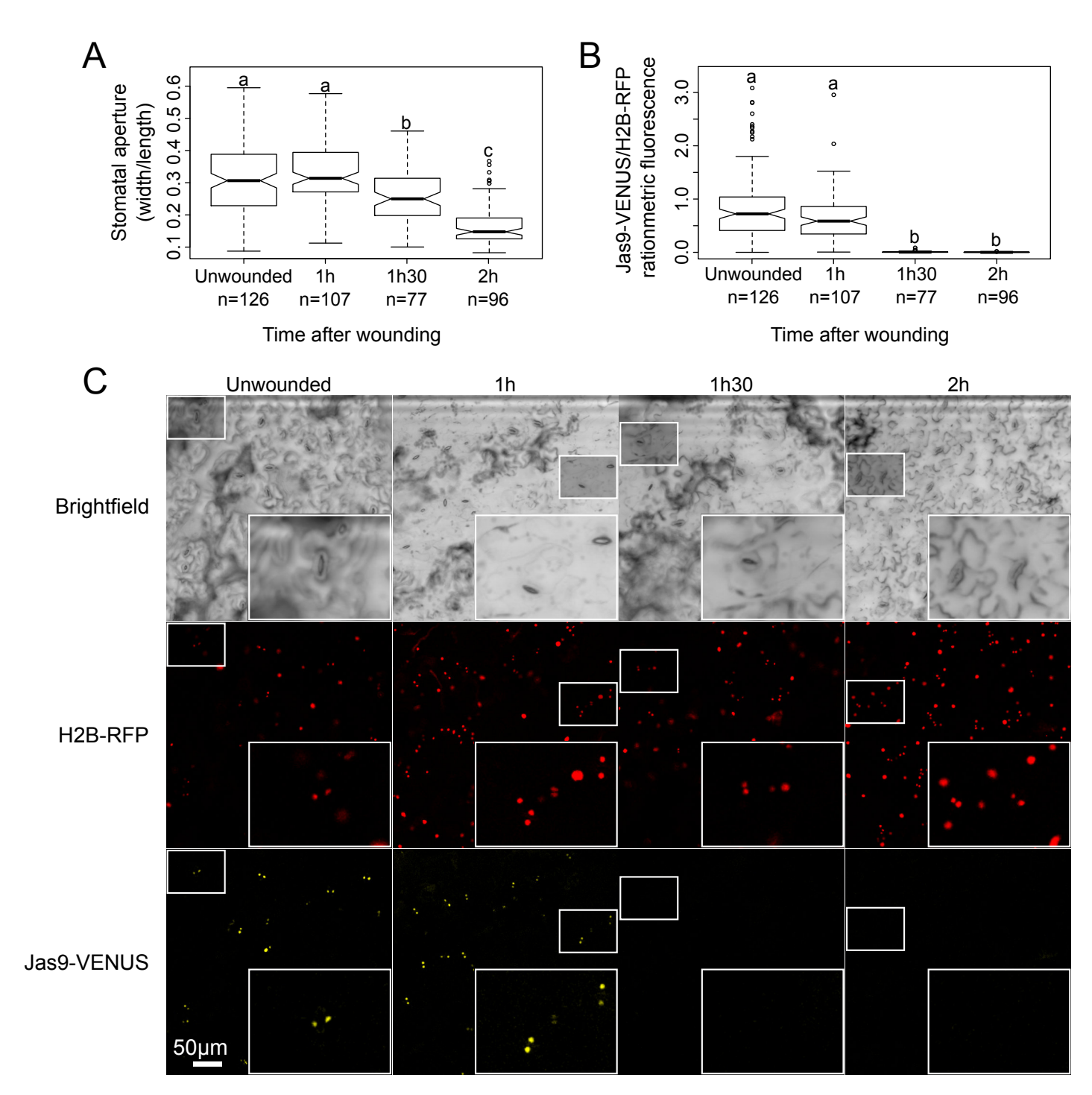
A
Stomatal aperture (width/length)
0.1 0.2 0.3 0.4 0.5 0.6
a
a
b
c
Unwounded n=126
1h n=107
1h30 n=77
2h n=96
Time after wounding
B
Jas9-VENUS/H2B-RFP rationmetric fluorescence
0.0 1.0 2.0 3.0
a
a
b
b
Unwounded n=126
1h n=107
1h30 n=77
2h n=96
Time after wounding
C
Unwounded
1h
1h30
2h
Brightfield
H2B-RFP
Jas9-VENUS
50µm

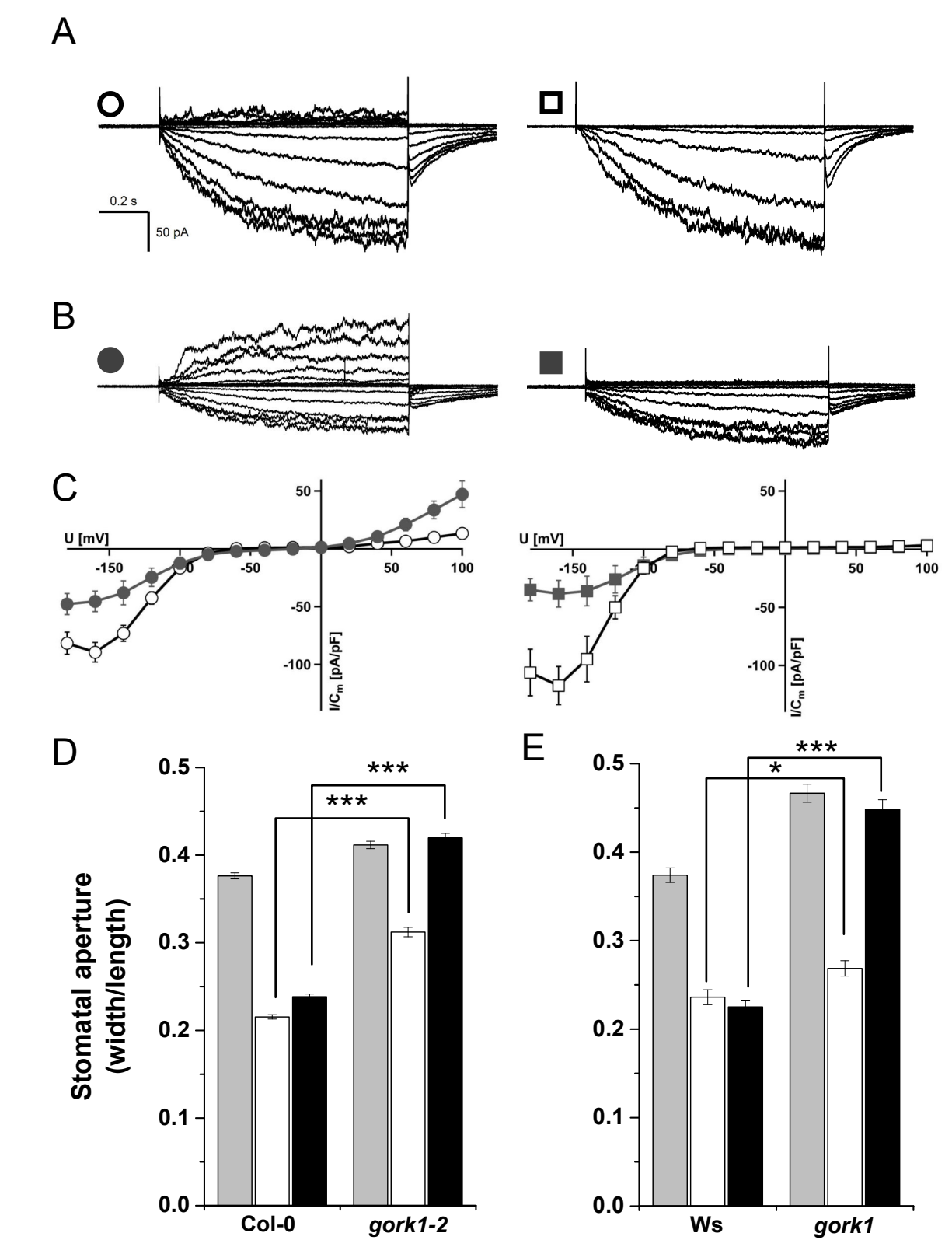
A
0.2 s
50 pA
B
C
U [mV]
-150
-50
50
100
50
-50
-100
I/C$_m$ [pA/pF]
D
Stomatal aperture (width/length)
0.5
0.4
0.3
0.2
0.1
0.0
***
***
Col-0
gork1-2
E
***
*
Ws
gork1

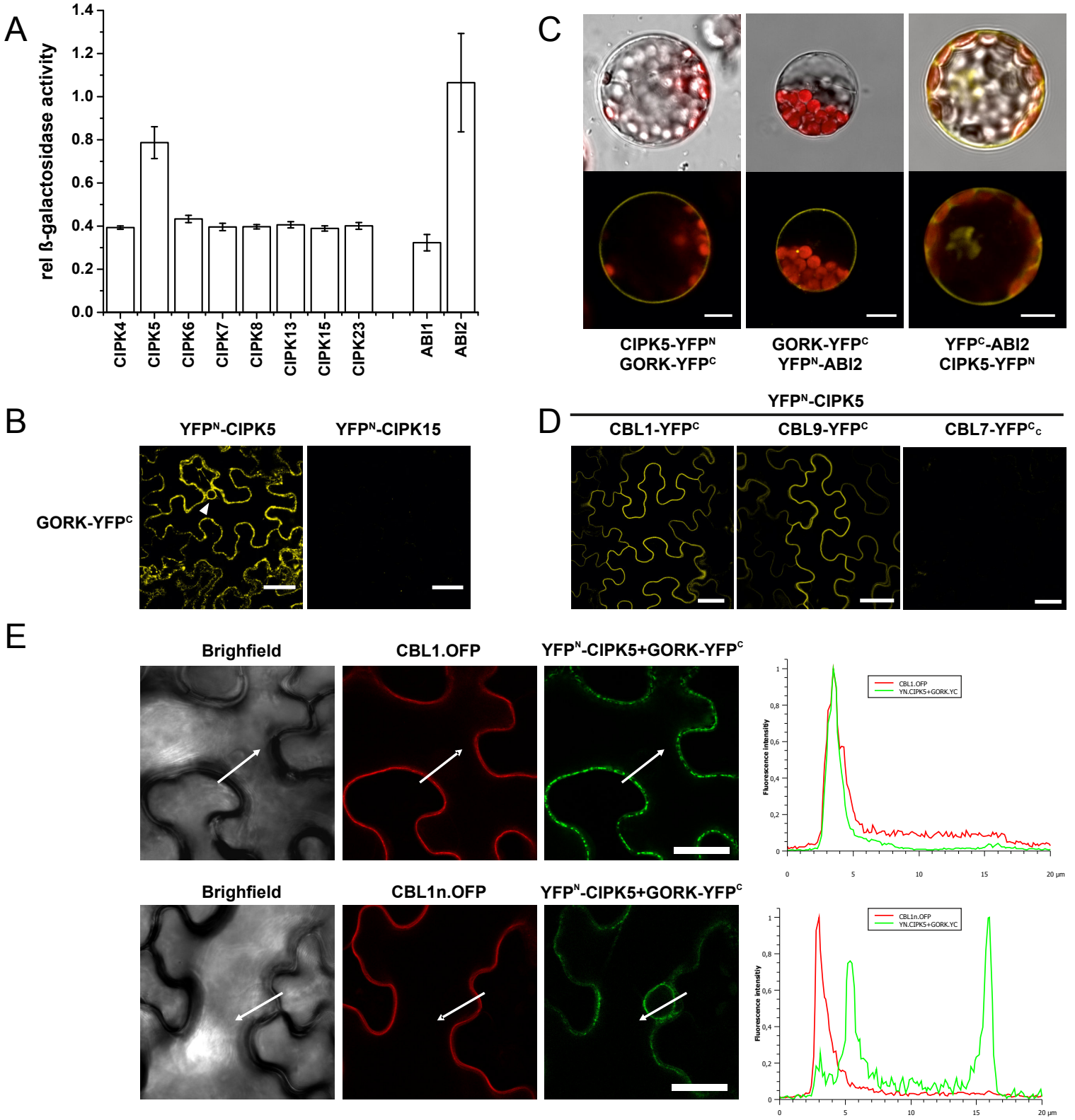
A
rel ß-galactosidase activity
1.4
1.2
1.0
0.8
0.6
0.4
0.2
0.0
CIPK4
CIPK5
CIPK6
CIPK7
CIPK8
CIPK13
CIPK15
CIPK23
ABI1
ABI2
C
CIPK5-YFPN
GORK-YFPC
GORK-YFPC
YFPN-ABI2
YFPC-ABI2
CIPK5-YFPN
B
YFPN-CIPK5
YFPN-CIPK15
GORK-YFPC
D
YFPN-CIPK5
CBL1-YFPC
CBL9-YFPC
CBL7-YFPC
E
Brighfield
CBL1.OFP
YFPN-CIPK5+GORK-YFPC
CBL1.OFP
YN.CIPK5+GORK.YC
Fluorescence intensity
Brighfield
CBL1n.OFP
YFPN-CIPK5+GORK-YFPC
CBL1n.OFP
YN.CIPK5+GORK.YC
Fluorescence intensity

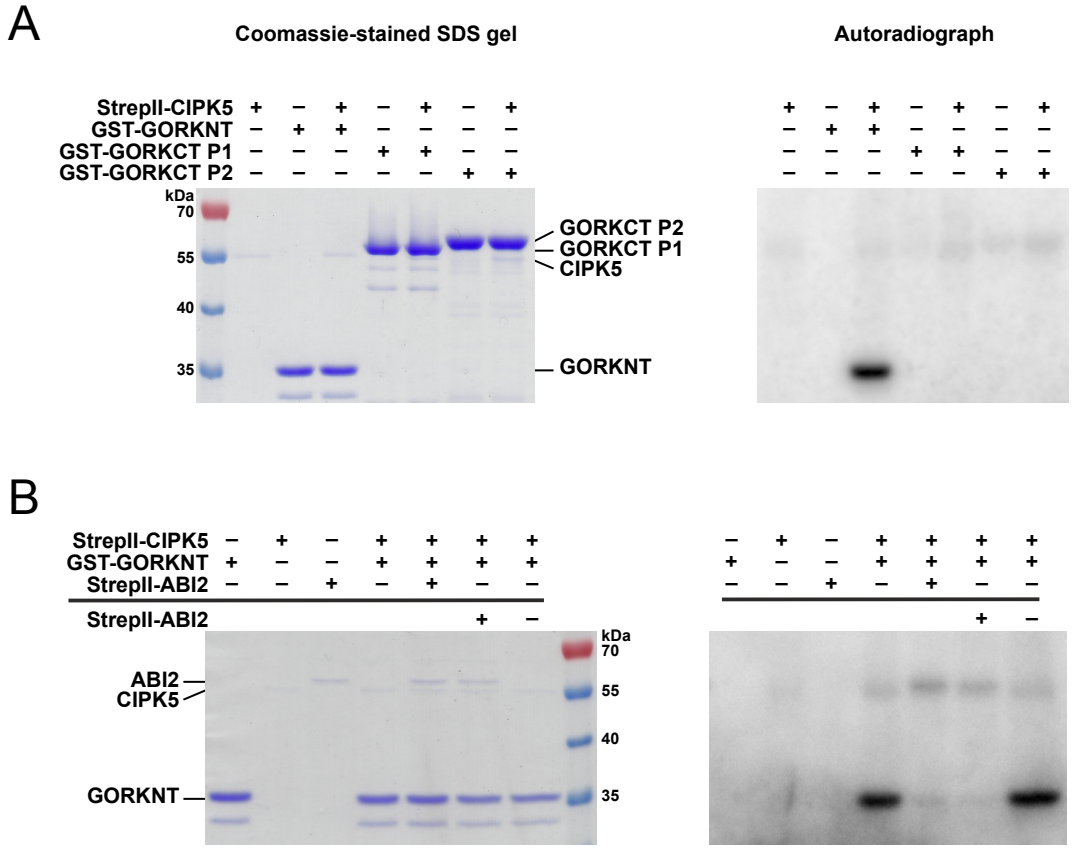
A
Coomassie-stained SDS gel
Autoradiograph
StrepII-CIPK5
GST-GORKNT
GST-GORKCT P1
GST-GORKCT P2
kDa
70
55
40
35
GORKCT P2
GORKCT P1
CIPK5
GORKNT
B
StrepII-CIPK5
GST-GORKNT
StrepII-ABI2
StrepII-ABI2
ABI2
CIPK5
GORKNT
kDa
70
55
40
35

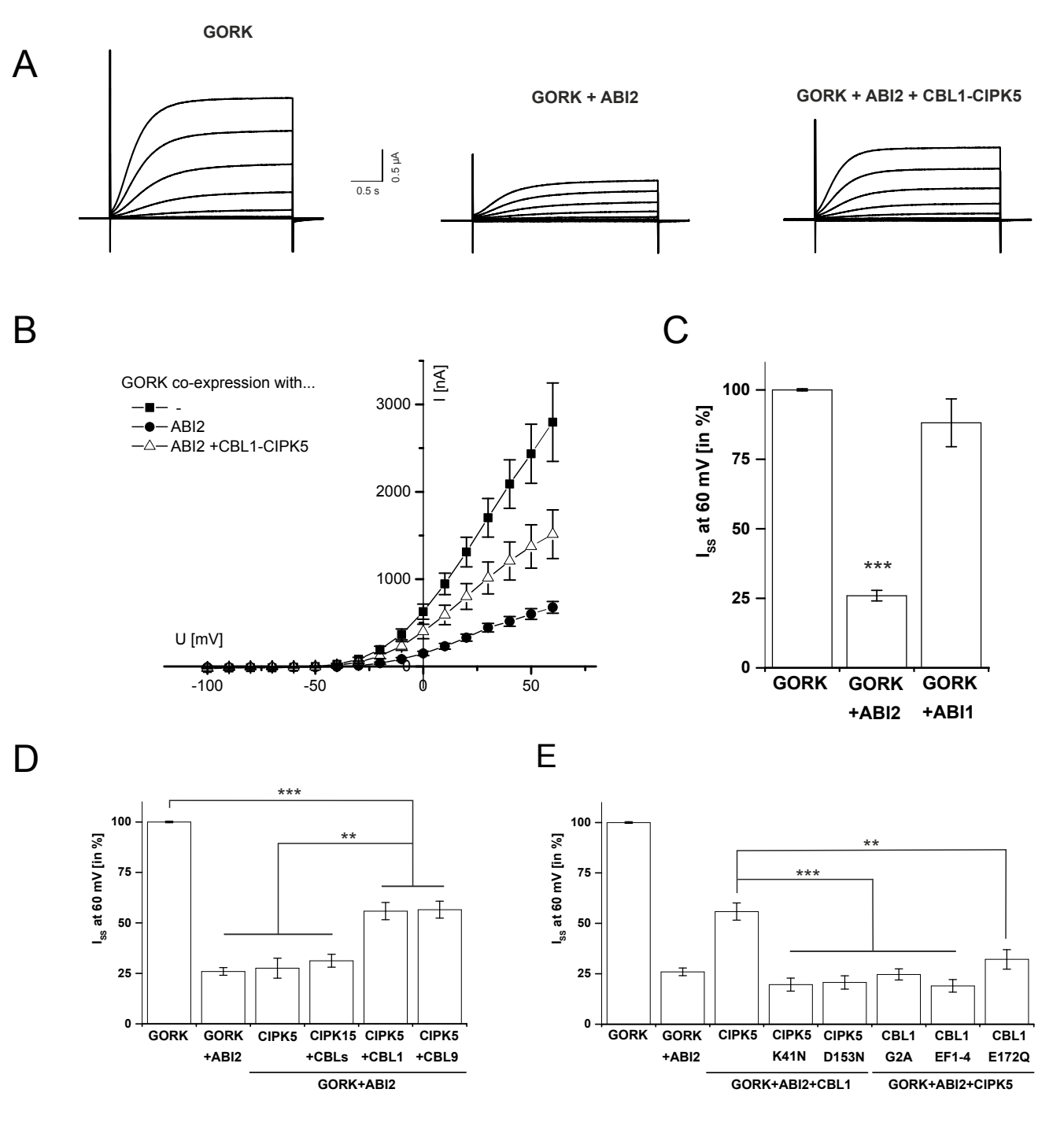
A
GORK
GORK + ABI2
GORK + ABI2 + CBL1-CIPK5
0.5 µA
0.5 s
B
GORK co-expression with...
-
ABI2
ABI2 +CBL1-CIPK5
I [nA]
U [mV]
3000
2000
1000
0
-100
-50
0
50
C
$I_{ss}$ at 60 mV [in %]
100
75
50
25
0
***
GORK
GORK +ABI2
GORK +ABI1
D
$I_{ss}$ at 60 mV [in %]
***
**
GORK
GORK +ABI2
CIPK5
CIPK15 +CBLs
CIPK5 +CBL1
CIPK5 +CBL9
GORK+ABI2
E
$I_{ss}$ at 60 mV [in %]
**
***
GORK
GORK +ABI2
CIPK5
CIPK5 K41N
CIPK5 D153N
CBL1 G2A
CBL1 EF1-4
CBL1 E172Q
GORK+ABI2+CBL1
GORK+ABI2+CIPK5

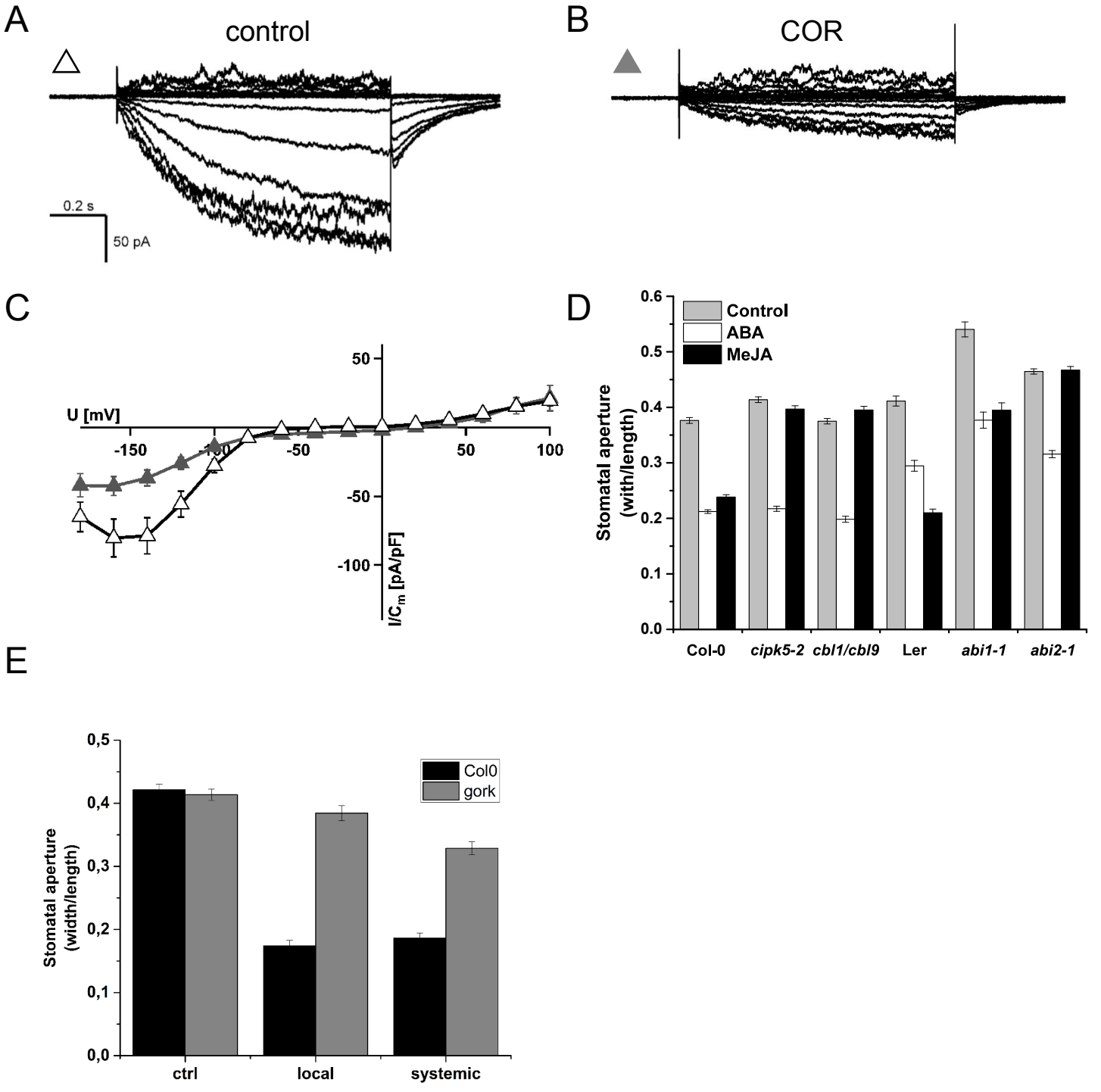
A
control
0.2 s
50 pA
B
COR
C
U [mV]
-150
-100
-50
50
100
50
-50
-100
I/C_m [pA/pF]
D
Control
ABA
MeJA
Stomatal aperture (with/length)
0.0
0.1
0.2
0.3
0.4
0.5
0.6
Col-0
cipk5-2
cbl1/cbl9
Ler
abi1-1
abi2-1
E
Col0
gork
Stomatal aperture (width/length)
0,0
0,1
0,2
0,3
0,4
0,5
ctrl
local
systemic

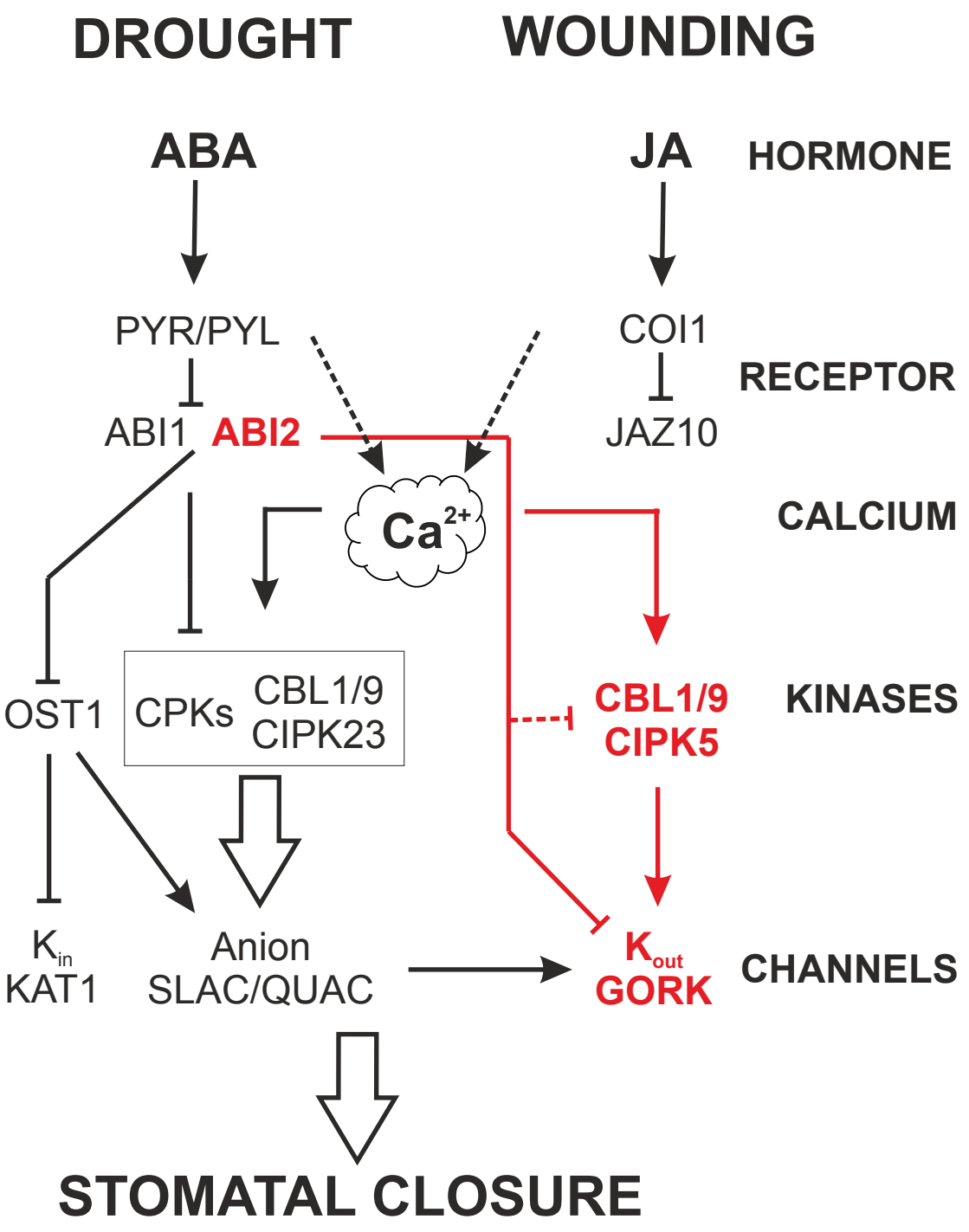
DROUGHT
WOUNDING
ABA
JA
HORMONE
PYR/PYL
COI1
RECEPTOR
ABI1
ABI2
JAZ10
Ca2+
CALCIUM
OST1
CPKs
CBL1/9
CIPK23
CBL1/9
CIPK5
KINASES
Kin
KAT1
Anion
SLAC/QUAC
Kout
GORK
CHANNELS
STOMATAL CLOSURE

# Figure S1

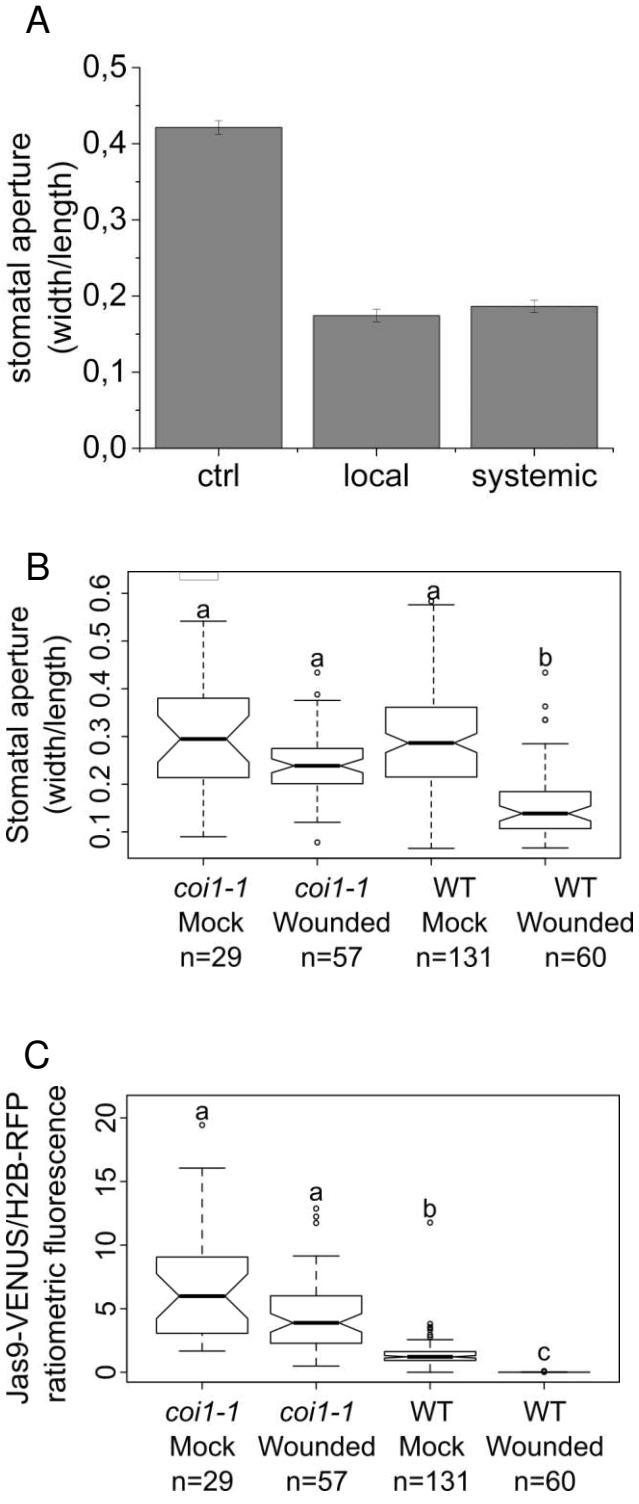


**Figure S1. Wounding induces local and systemic, JA dependent guard cell responses. Related to Fig. 1 and 2**

A) Stomatal aperture assays of wildtype Col-0. Guard cells were pre-opened in the light for 2 h, then control apertures were measured and one leaf per plant was mechanically wounded using forceps. Apertures were determined on excised leaves after 1h as the ratio of stomatal width to length. Systemic leaf was in position +3 of the local leaf. Averages from three or more independent experiments (≥ 80 stomata per bar) are shown. Error bars represent S.E.

B) Boxplot showing stomatal apertures in response to wounding of wildtype Col-0 and *coi1-1* homozygous mutants expressing the JA-sensor p35S::Jas9-Venus-N7. Epidermal strips were taken from the abaxial side of leaves that were unwounded (mock) or mechanically wounded using forceps.

C) Boxplot showing the ratiometric quantification of Jas9-VENUS/H2B-RFP fluorescence of epidermal strips shown in (B) indicative for JA signaling efficiency. The experiment was repeated 3 times with similar results. Boxplots show data for one representative experiment in B and C.

Figure S2

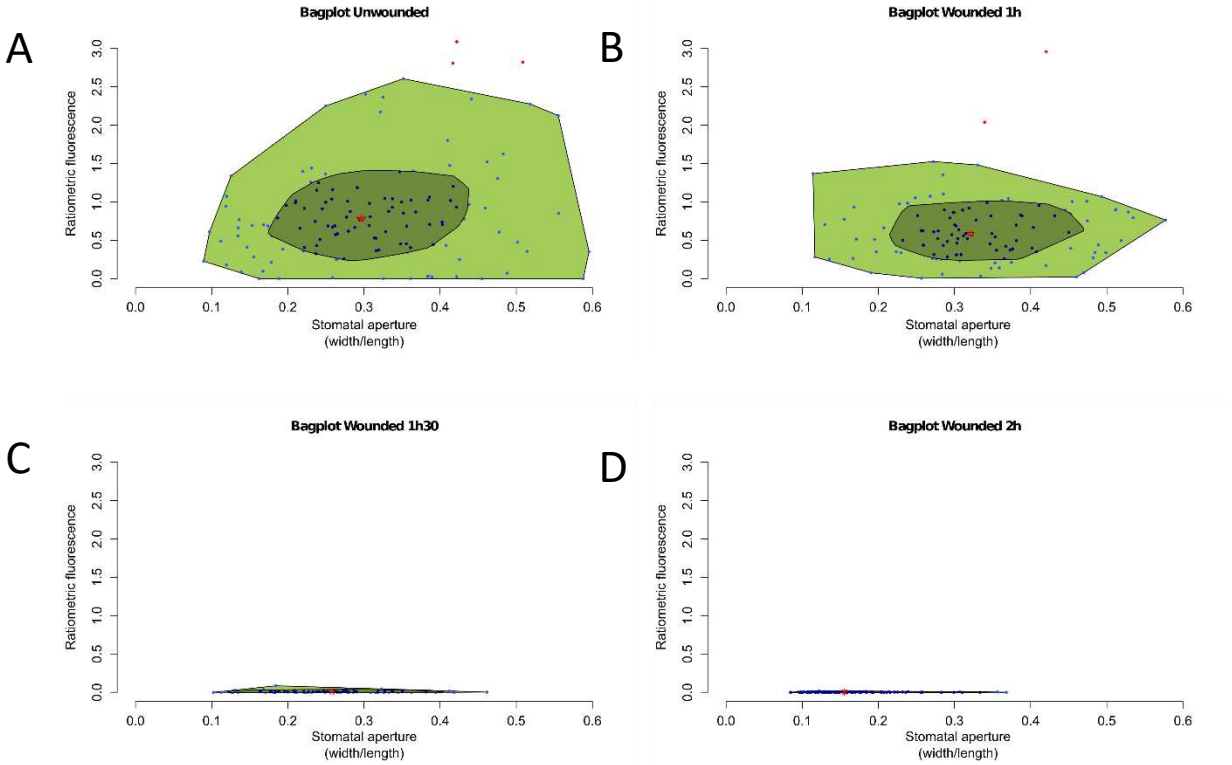


**Figure S2. Correlation of Jas9-VENUS fluorescence and stomatal aperture. Related to Fig. 1 and 2**

Bagplots showing the relation between the guard cell ratiometric Jas9-VENUS/H2B-RFP fluorescence and stomatal aperture of unwounded (A) and wounded (B – D) leaves. They allow to visualize the spread, skewness, and outliers of the data set used, particularly in the unwounded condition. While the ratiometric fluorescence is clearly less spread after 1 hour it is not the case for stomata opening even after 1h 30 minutes. Data used is the same as on Fig. 1. The inner polygon ("bag") contains 50% of all data points. The outer polygon ("loop") contains all points that are not marked as outliers. Dark blue, light blue and red dots represent data points contained within the bag, the loop or marked as outliers, respectively. The asterisk symbol represent the depth median (i.e. the two dimensional analog of the median that is used in the one-dimensional boxplots on Fig. 1).

Figure S3

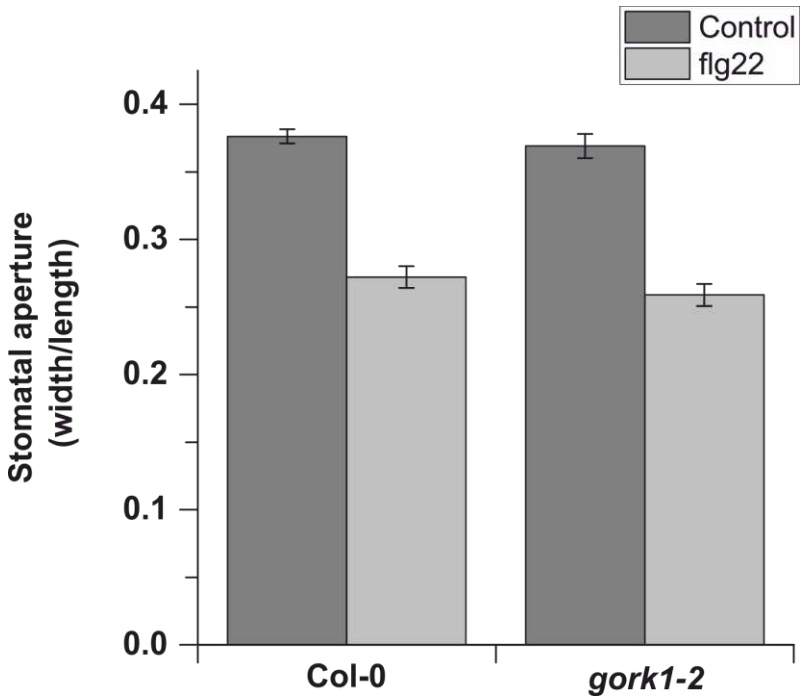


**Figure S3. Stomatal closure in response to flg22 is unaffected in *gork1-2* guard cells. Related to Fig. 2**

Guard cell responses of the *gork1-2* mutant towards the bacterial elicitor flg22 show that GORK is not involved in flagellin induced stomatal closure. Stomata were pre-opened under light for 2 h and subsequently incubated with 5 µM flg22 for 1 h. Averages from two or more independent experiments (≥ 80 stomata per bar) are shown. Error bars represent S.E.

Figure S4

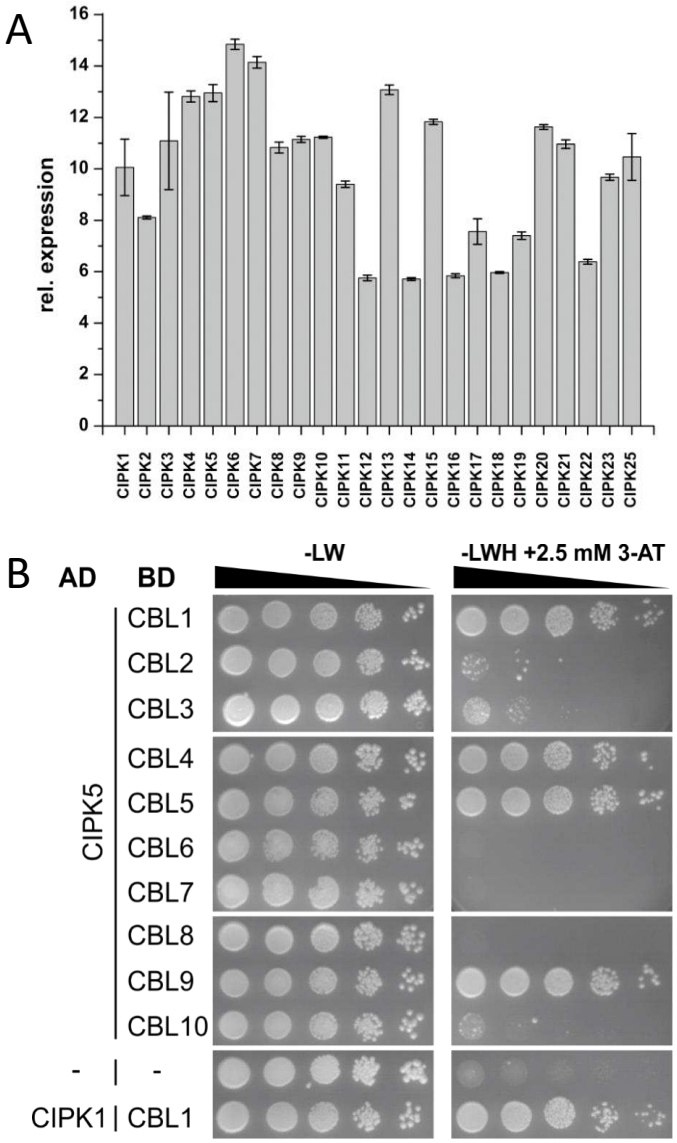


**Figure S4. Expression profile of CIPKs in guard cells and Y2H analysis CBL-CIPK5 interaction. Related to Fig. 3A**

(A) Expression profiles of CIPKs based on guard cell micro-array data (Bauer, et al., 2013). CIPKs exhibiting relative expression levels above 11 were considered for further analyses. The following AGI codes where checked: CIPK1 (AT3G17510), CIPK2 (AT5G07070), CIPK3 (AT2G26980), CIPK4 (AT4G14580), CIPK5 (AT5G10930), CIPK6 (AT4G30960), CIPK7 (AT3G23000), CIPK8 (AT4G24400), CIPK9 (AT1G01140), CIPK10 (AT5G58380), CIPK11 (AT2G30360), CIPK12 (AT2G30360), CIPK13 (AT4G18700), CIPK14 (AT2G34180), CIPK15 (AT5G01810), CIPK16 (AT2G25090), CIPK17 (AT1G48260), CIPK18 (AT1G29230), CIPK19 (AT5G45810), CIPK20 (AT5G45820), CIPK21 (AT5G57630), CIPK22 (AT2G38490), CIPK23 (AT1G30270) and CIPK25 (AT5G25110).

(B) The CIPK5 protein strongly interacts with CBL1, CBL4, CBL5 and CBL9 in yeast. Dilution series of the yeast strain PJ69-4A, transformed with the indicated combinations of activation domain (AD) and DNA-binding domain (BD) plasmids, were spotted on SD media without Leu and Trp (-LW; selection for positive transformants) or without Leu, Trp and His (-LWH and 2.5 mM 3-amino-1,2,4-triazole; selection for interaction), and incubated for 7 days at 30 °C. The published interaction of AD-CIPK1 and BD-CBL1 was used as a positive control.

Figure S5

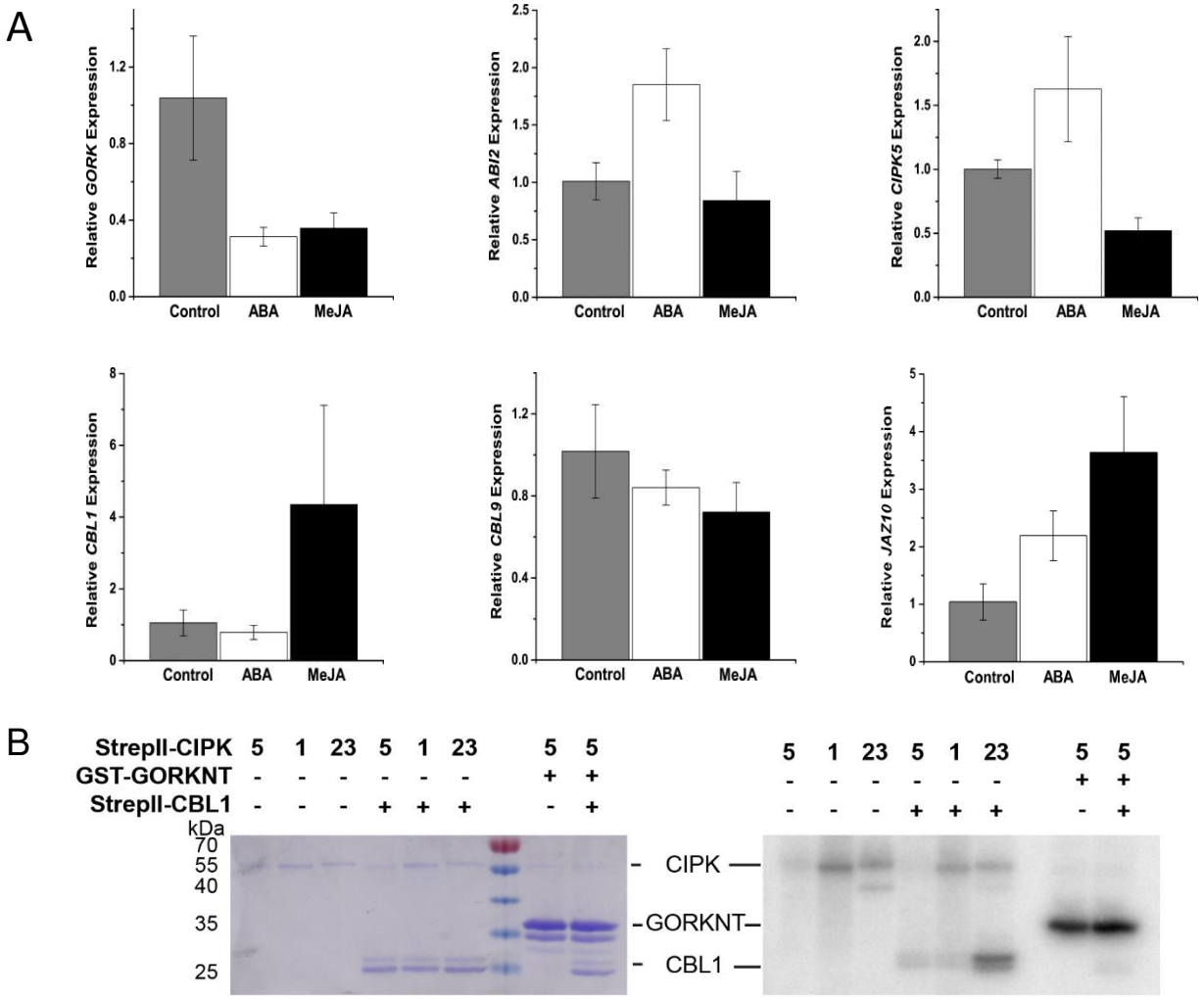


**Figure S5. qPCR analysis of *GORK, ABI2, CIPK5, CBL1, CBL9* and *JAZ10* in guard cells, effect of CBL1 on CIPK5 autophorsphorylation and GORK phosphorylation efficacy. Related to Fig. 2, 3 and 4**

A) Expression of *GORK* is reduced upon both ABA and MeJA treatment, indicating a possible negative regulation. Both *ABI2* and *CIPK5* expression are upregulated after ABA but downregulated after MeJA, whereas *CBL1* is strongly expressed upon MeJA treatment. This implicates possible different regulatory mechanisms for the respective regulators of GORK channel activity. *CBL9* expression was mildly downregulated upon both ABA and MeJA treatment, highlighting different properties in regulation and specificity of the two proteins. The JA expression marker JAZ10 was induced upon both ABA and MeJA, with the stronger induction in the latter condition. Change of relative expression in stomata after 2h upon spray treatment with 50 µM (±)-ABA or 25 µM MeJA. Transcript amounts were standardized to UBC21 transcripts and displayed relative to the expression level in the control treatment. Bars represent means of at least three guard cell samples (± S.D.), measured in three technical replicates.

B) Autophosphorylation of CIPK5, CIPK1 and CIPK23, as well as phosphorylation of GST-tagged GORK N-terminal domain (amino acids 1 to 67; GST-GORKNT) was analyzed by in vitro kinase assay. All reactions were performed in presence and absence of 1 µg of recombinant StrepII-CBL1 protein. The figure shows a scan of the coomassie stained SDS-PAGE (left) and the autoradiography (right).

Figure S6

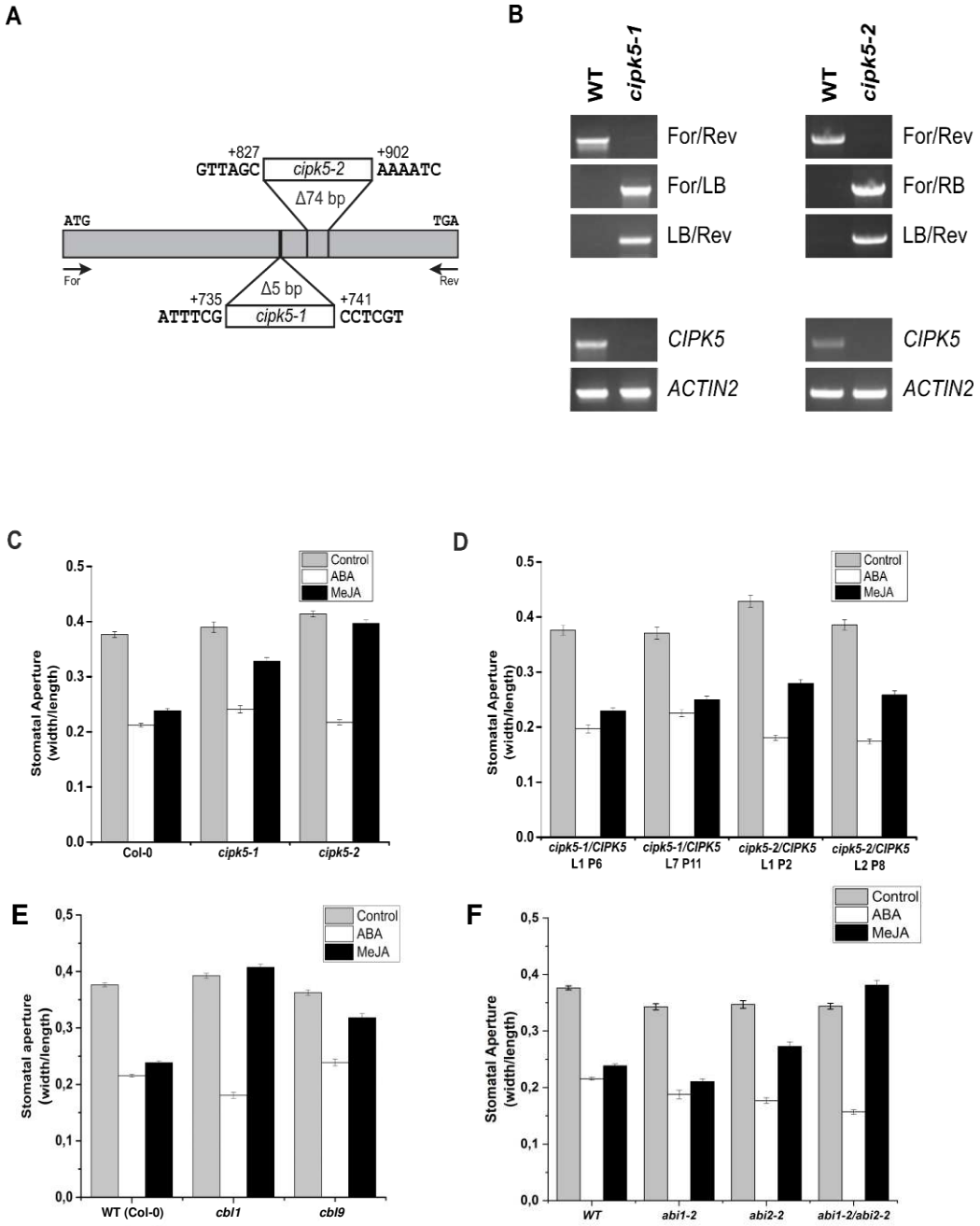


**Figure S6. Stomatal responses of *cipk5*, *cbl1* and *cbl9* mutants. Related to Fig. 6**

A) Structure of the T-DNA insertional alleles SALK_063555 (*cipk5-1*) and SALK_084455 (*cipk5-2*) of the *CIPK5* gene (At5g10930). In allele *cipk5-1*, T-DNA was inserted behind nucleotide 735, downstream of the start codon and caused a 5 bp sequence deletion. Here, a double T-DNA insertion took place with their left borders adjacent to the *CIPK5* sequence. In allele *cipk5-2*, the T-DNA integrated at position +828, leading to a sequence deletion of 74 bp. The position of primer For and Rev (used for T-DNA border analysis) is depicted.

B) PCR analyses of the T-DNA insertion in homozygous *cipk5-1* and *cipk5-2* plants, and in wildtype plants as control with indicated primer pairs (top). RT-PCR transcript analyses in *cipk5-1*, *cipk5-2* and wildtype indicated that T-DNA insertion in both *cipk5* mutants reduces *CIPK5* transcript to an undetectable level (bottom). *ACTIN2* expression was analyzed as quantification control.

C - E) Guard cell responses of independent *cipk5* T-DNA mutants (C) and complementation lines (D) towards ABA or MeJA. (E) Stoma assays of *cbl1* and *cbl9* mutants in response to ABA or MeJA. Stomata were pre-opened under light for 2 h, then incubated with 20 µM (±)-ABA or 10 µM MeJA for 1 h. Averages from three or more independent experiments (≥ 80 stomata per bar) are shown. Error bars represent S.E. (F) Stoma assays of ABI1 and ABI2 single and double T-DNA insertion mutants. Experimental conditions were as in (E).

Figure S7

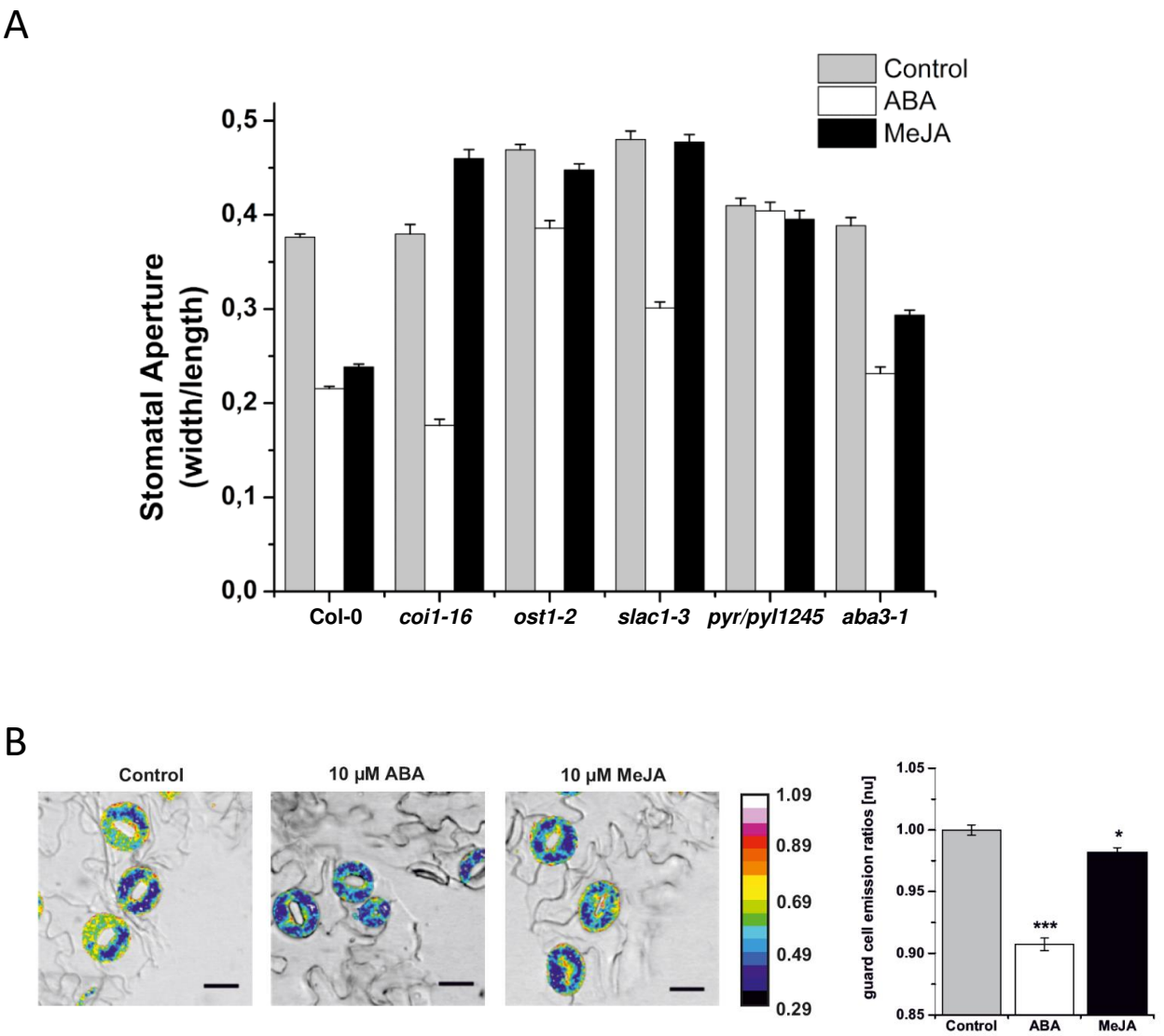


**Figure S7. Cross-talk of JA and ABA. Related to Fig. 6**

(A) Stoma assays of *coi1-16, ost1-2, slac1-3, pyr/pyl1245 and aba3-1* in response to ABA or MeJA. Stomata were pre-opened under light for 2 h, then incubated with 20 µM (±)-ABA or 10 µM MeJA for 1 h. Averages from three or more independent experiments (≥ 80 stomata per bar) are shown. Error bars represent S.E.

(B) ABA concentration changes visualized using the ABAleon reporter system. Increased ABA levels are reported by a decrease in the emission ratio of the FRET sensor. Representative images of guard cells (in false colors) pre-incubated for 1 h with either methanol (control), 10 µM (+)-ABA or 10 µM MeJA. ABA-treated guard cells exhibited significantly increased ABA levels, while the effect of MeJA on cytosolic guard cell ABA concentration was less pronounced. Bars represent mean values with S.E. (n ≥ 214). Asterisks depict significance levels.

# Supplemental Tables

S1. Adjusted p-values for stomatal opening measurements in Fig. 1

| | Unwounded | 1h | 1h30 |
|---|---|---|---|
| 1h | 0.0872 | - | - |
| 1h30 | 0.0067 | 4.2e-5 | - |
| 2h | <2e-16 | <2e-16 | 2.5e-8 |

S2. Adjusted p-values for Jas9-VENUS/H2B-RFP ratiometric fluorescence measurements in Fig. 1

| | Unwounded | 1h | 1h30 |
|---|---|---|---|
| 1h | 0.41 | - | - |
| 1h30 | <2e-16 | <2e-16 | - |
| 2h | <2e-16 | <2e-16 | 0.41 |

S3. qPCR primers, related to KRT

| **Gene** | **AGI code** | **Seq fwd** | **Seq rev** |
|---|---|---|---|
| ABI2 | AT5G57050 | GGACTTAGAGGCTATTG | AGGATTAAATCCATTAGTG |
| CBL1 | AT4G17615 | AAATTAGAGTGGAGTGAT | TGATTACACCGATTAGC |
| CBL9 | AT5G47100 | GATAAGACAGAATGGAGC | CCTACGACTTGGTCTCTA |
| CIPK5 | AT5G10930 | AATTTCCGCCGTGGTT | CGGCGATATCGGCTCT |
| GORK | AT5G37500 | GATACTCAGACCTACCG | CCAAGTGTAACCTTCG |
| JAZ10 | AT5G13220 | ATCCCGATTTCTCCGGTCCA | ACTTTCTCCTTGCGATGGGAAGA |
| UBC21 | AT5G25760 | CAGTCTGTGTGTAGAGCTATCATAGCAT | AGAAGATTCCCTGAGTCGCAGTT |